AD-768 034

ESTIMATION OF THE AVERAGE FREQUENCY OF A RANDOM PROCESS

John Joseph Herro

Chicago University

Prepared for:

Office of Naval Research

May 1973

Unclassified
Security Classification

AD 768034

DOCUMENT CONTROL DATA - R & D

(Security classification of title, body of abstract and indexing annotation must be entered when the overall report is classified)

1. ORIGINATING ACTIVITY (Corporate author) Laboratory for Atmospheric Probing Department of Geophysical Sciences The University of Chicago	2a. REPORT SECURITY CLASSIFICATION Unclassified 2b. GROUP N/A

3. REPORT TITLE

Estimation of the Average Frequency of a Random Process

4. DESCRIPTIVE NOTES (Type of report and inclusive dates)
Technical Report

5. AUTHOR(S) (First name, middle initial, last name)

John Joseph Herro

6. REPORT DATE May 1973	7a. TOTAL NO. OF PAGES ~~120~~ 71	7b. NO. OF REFS 12
8a. CONTRACT OR GRANT NO. N00014-67A-0285-0014 b. PROJECT NO. NR 061-188 c. d.	9a. ORIGINATOR'S REPORT NUMBER(S) Technical Report No. 31 9b. OTHER REPORT NO(S) (Any other numbers that may be assigned this report)	

10. DISTRIBUTION STATEMENT

Approved for public release; distribution unlimited.

11. SUPPLEMENTARY NOTES	12. SPONSORING MILITARY ACTIVITY Office of Naval Research (Code 438) Department of the Navy Arlington, Virginia 22217

13. ABSTRACT

The purpose of this work is to develop a means of estimating, in real time, the average frequency of a random process, given only a time-limited sample of that process. The average frequency of a random process is defined in terms of the power spectral density. Previous estimators of average frequency were mathematically based on estimating the power spectral density. In this work, the average frequency is expressed in terms of the autocorrelation and cross-correlation functions, and a new estimator is obtained which is based on estimates of these correlation functions. Two estimators presented in the literature and the proposed estimator are compared, and expressions are obtained for the power spectral density and autocorrelation function at each point in the systems, exclusive of the outputs. Approximate expressions are obtained for the bias and variance of the proposed estimator and one of the referenced estimators. A lab. model of the proposed device was constructed and tested under several sets of operating conditions. It is found that, under typical operating conditions, the proposed estimator performs almost as well as those proposed earlier, and is simpler in form. For every short samples of the random process, however, the difference in variance becomes more noticeable.

Key words: Power Spectral Density, Average Frequency Estimators, Simulation

DD FORM 1 NOV 65 1473

Security Classification

AGO 5698A

AD 768034

THE UNIVERSITY OF CHICAGO

DEPARTMENT OF THE GEOPHYSICAL SCIENCES

AND

ILLINOIS INSTITUTE OF TECHNOLOGY

DEPARTMENT OF ELECTRICAL ENGINEERING

TECHNICAL REPORT NO. 31

LABORATORY FOR ATMOSPHERIC PROBING

ESTIMATION OF THE AVERAGE FREQUENCY OF A RANDOM PROCESS* †

by

JOHN JOSEPH HERRO

Chicago, Illinois

May, 1973

*Submitted in partial fulfillment of the requirements for the degree of Doctor of Philosophy in Electrical Engineering in the Graduate School of Illinois Institute of Technology.

†Research supported in part by the Office of Naval Research under Contract ONR-N00014-67A-0285-0014.

ABSTRACT

The purpose of this work is to develop a means of estimating, in real time, the average frequency of a random process, given only a time-limited sample of that process. Motivation for this study is found in the field of radar meteorology. In a rainstorm, the velocity of each falling raindrop is a direct function of its size. If the rainstorm is observed with a Doppler radar, the average frequency of the return signal gives the meteorologist useful information about the sizes of the raindrops present.

The average frequency of a random process is defined in terms of the power spectral density. Previous estimators of average frequency were mathematically based on estimating the power spectral density. In this work, the average frequency is expressed in terms of the auto-correlation and cross-correlation functions, and a new estimator is obtained which is based on estimates of these correlation functions.

Two estimators presented in the literature and the proposed estimator are compared, and expressions are obtained for the power spectral density and autocorrelation function at each point in the systems, exclusive of the outputs. Approximate expressions are obtained for the bias and variance of the proposed estimator and one of the referenced estimators.

A laboratory model of the proposed device was constructed and tested under several sets of operating conditions. It is found that, under typical operating conditions, the proposed estimator performs almost as well as those proposed earlier, and is simpler in form. For very short samples of the random process, however, the difference in variance becomes more noticeable.

The following conclusions can be drawn:

While previous estimators of average frequency resulted from estimates of the power spectral density, a new, simpler estimator can be derived from estimates of autocorrelation and cross-correlation functions.

In each estimator considered, the autocorrelation and cross-correlation functions at each point exclusive of the output are expressible in terms of these same functions at the input. For the proposed estimator and a previous estimator, the bias and variance can be expressed, approximately, in terms of the input autocorrelation function. For the two estimators, corresponding expressions contain many similar terms.

For very long samples of the random process, all estimators considered are asymptotically perfect.

The proposed estimator, while simpler and easier to construct then previous ones, has about the same variance as the others under typical operating conditions, and should, therefore, find use in radar meteorology.

FOREWORD

This report is a reprint of the Ph.D. dissertation of John J. Herro who received his Ph.D. degree in Electrical Engineering from Illinois Institute of Technology in May 1973. This is the fourth Ph.D. topic at IIT which has originated from the association between the University of Chicago and Illinois Institute of Technology in their joint operation of the Laboratory for Atmospheric Probing.

The work presented here provides further insight to the mean frequency estimation problem, a problem fundamental to radar meteorology and one which has assumed increased importance due to recent advances in real time multigate digital processing. Herro's work adds to our understanding of the operation of such devices and as such is a valuable contribution to the rapidly advancing field of Doppler Radar Meteorology.

Robert J. Serafin
Research Engineer

Lester C. Peach
Associate Director

R C Srivastava

Ramesh C. Srivastava
Acting Director
Laboratory for Atmospheric Probing

ACKNOWLEDGEMENTS

The author wishes to thank his thesis adviser, Dr. Lester C. Peach, for his technical direction, encouragement, and guidance in the preparation of this work.

Acknowledgement is made to the Illinois Institute of Technology, The University of Chicago, the National Science Foundation for their financial assistance. The University of Chicago support was through the Office of Naval Research.

Additional thanks are extended to Dr. Robert J. Serafin for his constructive criticism and suggestions, and to Dr. Kenneth W. Haag for his assistance in the design and construction of the laboratory model.

The author thanks Mrs. Marie Mikulskis and Mrs. Barbara Tekiela for their diligent typing of the manuscript.

Finally, the author is most grateful to his parents, Mr. and Mrs. Alexander C. Herro, for their encouragement, understanding, and patience during the course of his studies and research.

TABLE OF CONTENTS

TABLE OF CONTENTS
(continued)

TABLE OF CONTENTS
(continued)

LIST OF TABLES

LIST OF ILLUSTRATIONS

LIST OF ILLUSTRATIONS
continued

LIST OF SYMBOLS AND ABBREVIATIONS

Symbol	Definition
a	lower frequency limit of flat input spectrum
a,b	two general, linear, time-invariant networks
A - W	designating different points on the various estimators (see Figs. 4-6)
$A_1 - A_4$	areas
A.E.F.	Average Extraction Filter
b	upper frequency limit of flat input spectrum
B	bandwidth of the low-pass filters
Buf.	buffer
$C_1 - C_3$	capacitors
D	denominator voltage in millivolts
db	decibels
deg	degrees
Div.	division
D.V.M.	digital voltmeter
$E[\ ]$	expected value of the quantity in brackets
f	frequency
$\bar{f}$	average frequency
FFT	Fast Fourier Transform
f_{LO}	frequency of the local oscillator
h(t)	impulse response of a linear, time-invariant network
$H(j\omega)$	transfer function of a linear, time-invariant network
Hz	Hertz, cycles per second

LIST OF SYMBOLS AND ABBREVIATIONS
continued

Symbol	Definition
i, j	indices of a double summation
j	$\sqrt{-1}$
J	Jacobian determinant
k	designating a particular member of an ensemble
k	index of a power series
lim	limit
L.O.	Local Oscillator
L.P.F.	Low Pass Filter
msec	millisecond
N	numerator voltage in millivolts
OSC.	oscillator
p	probability density function
P	power of the input waveform
$R_1 - R_3$	resistors
$R_{x1\,x2}(\tau)$	if subscripts are identical, ensemble autocorrelation function; otherwise, ensemble cross-correlation function
$\mathcal{R}_{x1\,x2}(\tau)$	if subscripts are identical, time autocorrelation function; otherwise, time cross-correlation function
$r(\tau)$	error in the estimate of $R(\tau)$
S(f), $S(\omega)$	power spectral density
sec	second
S/N	signal-to-noise (ratio)

LIST OF SYMBOLS AND ABBREVIATIONS
continued

Symbol	Definition
t	time
T	length of time-limited sample of the random process
θ	$T/2$
$v(t)$	voltage as a function of time
$v_1 - v_4$	divider input voltages at particular times
$v_{BT}(t)$	voltage at the output of Ciciora's filter due to a time-limited input
$V_T(2\pi f)$	Fourier transform of a time-limited input
$W(\omega)$	$\equiv 1$ for $\omega < 0$; $\equiv -1$ for $\omega > 0$
$x(t)$	any general function of time
x_a, x_b	inputs of general, linear, time-invariant networks a and b, respectively
$x_1 - x_4$	four general, gaussian random variables
X	designating a point on Fig. 7
y_a, y_b	outputs of general, linear, time-invariant networks a and b, respectively
$y_1 - y_4$	random variables resulting from a fourth-order transformation of random variables v_1 through v_4
$z(t)$	analytic signal associated with $x(t)$
α, β	the two outputs of the quadrature detector such that, for real input, $\beta = \check{\alpha}$
δ	Dirac delta function, unit impulse

LIST OF SYMBOLS AND ABBREVIATIONS
continued

Symbol	Definition
ϕ	phase
τ	argument of autocorrelation functions and cross-correlation functions, dummy argument of integration
ω	radian frequency
$(\hat{\ })$	estimate of a quantity
$(\dot{\ })$	derivative of a function
$(\ddot{\ })$	second derivative of a function
$(\check{\ })$	Hilbert transform of a function
$(\dot{\check{\ }})$	derivative of the Hilbert transform of a function
$(\ddot{\check{\ }})$	Hilbert transform of the second derivative of a function
$\equiv$	is equal to by definition
$\approx$	is approximately equal to
$*$	between two symbols, convolved with
$*$	as a superscript, complex conjugate
$\rightarrow$	approaches
Λ	covariance matrix
$\lvert\Lambda\rvert$	determinant of the covariance matrix
$\lvert\Lambda\rvert_{ij}$	$(i\text{-}j)^{th}$ cofactor, or signed minor, of the covariance matrix

CHAPTER I

INTRODUCTION

The purpose of this work is to develop a means of estimating, in real time, the average frequency of a random process. If $S(f)$ is the power spectral density of the process, the average frequency is defined by

$$\bar{f} = \frac{\int_0^\infty f\,S(f)\,df}{\int_0^\infty S(f)\,df} . \tag{1.1}$$

It is assumed that only a time-limited sample of the process is available. If it were available for all time, the average frequency could be known to any desired degree of accuracy and would not have to be estimated.

Motivation for this study is found in the field of radar-meteorology. Falling rain is observed with doppler radars. Because of air resistance, the downward velocity of each raindrop is a direct function of its size. Since the doppler shift in the reflection from each raindrop is directly proportional to its velocity, the size of a raindrop can be calculated from this shift.

In a rainstorm, reflections are received from many raindrops falling at different velocities, and thus the <u>aggregate</u> reflection from all these particles is a random process. Knowledge of the average frequency of this process gives the meteorologist useful information about the sizes of the

raindrops present. In general, only a limited time (typically one or two seconds) is available for each observation. At the end of this time, an estimate of the average frequency is desired.

A review of the literature on this subject appears in Chapter II. It is found that several estimators already exist. Of particular interest are those of Ciciora[2*] and Denenberg[5], because they provide real-time estimates of average frequency. This work introduces a new approach to the problem, leading to a proposed real-time estimator which is simpler than the previous ones.

In order to construct any of the devices to be considered here, the builder should know the signal bandwidth and dynamic range at each point in the system. This will enable him to specify suitable components for their construction. Therefore, a probabilistic analysis is performed on each of the estimators being considered, including the proposed one. Expressions for the autocorrelation function and power spectral density are obtained for every point in each system, up to but not including the output. Since the output in each system is obtained from a divider (compare equation (1.1)), no expression could be obtained for the autocorrelation function and power spectral density at that point.

Probabilistic analysis of the output divider was attempted. While the divider itself can be analyzed completely, a difficulty arises in trying to apply the analysis

---
*For all numbered references, see Bibliography.

to the devices under consideration. Therefore another device, similar to the proposed estimator, is introduced. It is designed specifically to enable the divider analysis to be applied. Although this "similar" device can be analyzed completely, no claim is made that it is equivalent to the proposed one. It is introduced solely to show how the divider analysis might be applied to a complete system.

For the case of a long observation time, it is found that a power series approximation to division can be made. By this method, approximate expressions are obtained for the bias and variance of the proposed estimator. For comparison, similar expressions are derived for Denenberg's estimator.

Since it is desired to compare the performance of the proposed estimator with that of the older, more complex devices, a laboratory model of the proposed device was constructed. Photographs of the waveforms at each point in the system are displayed. The new device is tested under several sets of typical operating conditions, and the variance of the estimate is compared with that of the other estimators.

CHAPTER II

REVIEW OF THE LITERATURE

Classical methods of estimating $\bar{f}$ involve estimating $S(f)$ and substituting this in (1.1). Thus

$$\hat{\bar{f}} = \frac{\int_0^\infty f\,\hat{S}(f)\,df}{\int_0^\infty \hat{S}(f)\,df} \tag{2.1}$$

where the caret (^) over a quantity denotes an estimate of that quantity. In one such method, the received signal is processed by an analog-to-ditigal converter, after which a digital computer uses the Fast Fourier Transform (FFT) algorithm to estimate $S(f)$. After $\hat{S}(f)$ is obtained from the F.T, $\hat{\bar{f}}$ is computed from (2.1).

A second method[12] is similar to the above in that it estimates $S(f)$ first and then calculates $\hat{\bar{f}}$. In this method, a bank of one hundred extremely selective filters is used to obtain $\hat{S}(f)$, the bandwidth of each filter being about 3 Hz. Again, $\hat{\bar{f}}$ is computed directly from (2.1).

Denenberg[5] takes a somewhat different approach. He developed an estimator for $\bar{f}$ which does not first estimate $S(f)$. In (2.1) above, Denenberg substitutes for $\hat{S}(f)$ a mathematical estimator called the periodogram. For the case of a simple time-limited sample of a real random process, the periodogram is as follows:

$$\hat{S}(f) = \frac{1}{T}\left|V_T(2\pi f)\right|^2 \tag{2.2}$$

where

$$V_T(2\pi f) = \int_0^T v_A(t)\,e^{-j2\pi ft}\,dt \tag{2.3}$$

and $v_A(t)$ is a particular sample function of the real random process and T is the observation time.

The right-hand side of (2.3) above is the Fourier transform of the time-limited version of $v_A(t)$. The periodogram $\hat{S}(f)$ is the power spectral density of this time-limited signal.

Using this estimate for $S(f)$, Denenberg shows that (2.1) is equivalent to

$$2\pi\hat{\bar{f}} = \frac{\int_0^T (\alpha\dot{\beta} - \beta\dot{\alpha})\,dt}{\int_0^T (\alpha^2 + \beta^2)\,dt} \tag{2.4}$$

where $\alpha(t) + j\beta(t)$ is the complex envelope of the random process. The functions $\alpha(t)$ and $\beta(t)$ are obtained from quadrature detection of the received signal. The dot represents differentiation with respect to time. A block diagram of Denenberg's estimator is shown in Fig. 1. Denenberg derived expressions for the variance of this estimator, which will be discussed in Chapter VI.

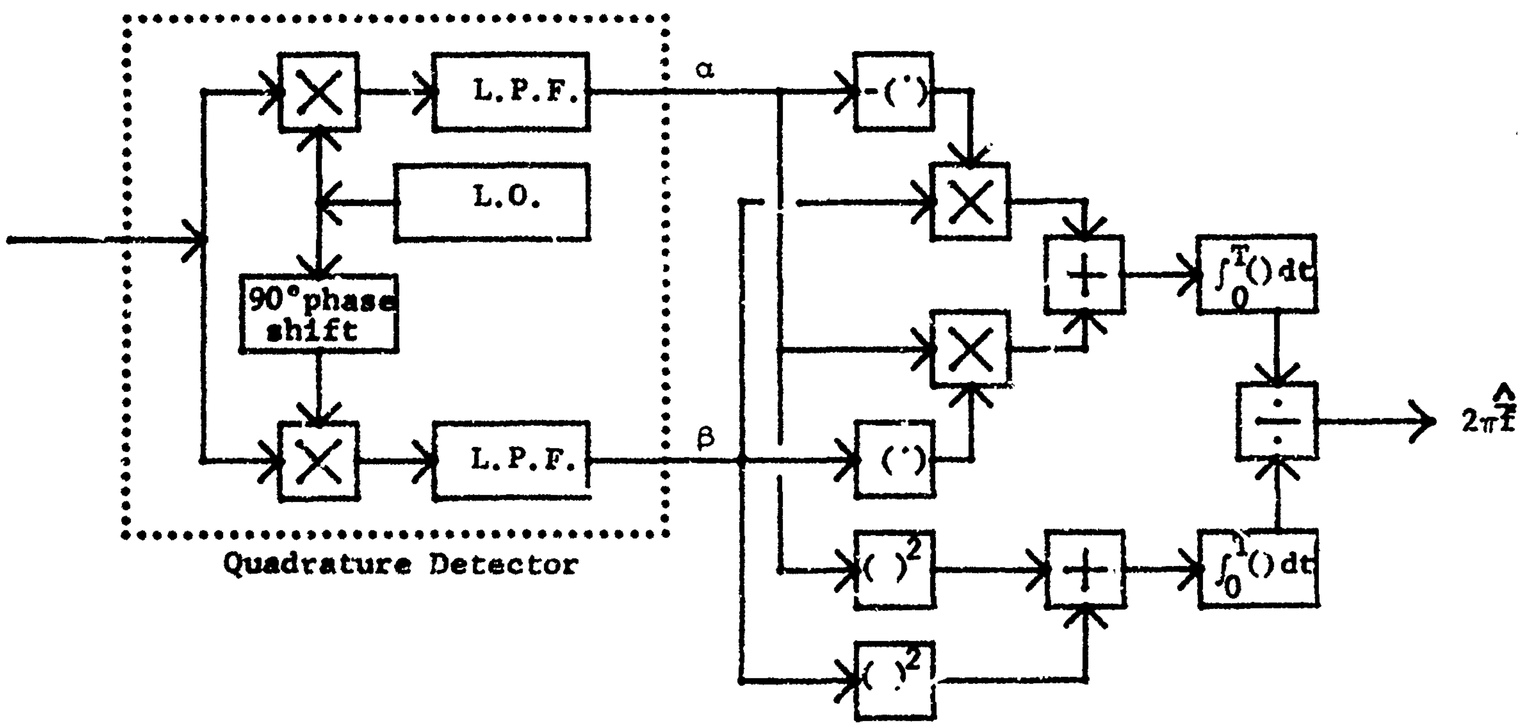

Fig. 1. Block Diagram of Denenberg's Estimator

Bello[1] proposes an estimator similar to Denenberg's. For the case of a rectangular window function, Bello's and Denenberg's estimators are identical.[6]

Miller and Rochwarger[9] investigate the problem of estimating $\bar{f}$ in the presence of additive, gaussian, colored noise. They derive expressions for the variance of the estimate. Since radar returns from rainstorms normally have excellent signal-to-noise ratios, noise in the received signal is not considered in this work.

Ciciora[2] takes a slightly different approach. Instead of multiplying $\hat{S}(f)$ by f as in (2.1), Ciciora passes the received signal through a filter which weights the signal with respect to frequency. For a single-frequency input, the amplitude of the output signal is proportional to the square root of the frequency. That is, the output <u>power</u> is proportional to the input frequency. The filter is a specialized version of the frequency discriminator commonly found in F.M. receivers. For simplicity, it can be assumed that

$$|H(j\omega)|^2 = |\omega| \qquad (2.5)$$

over the frequency range of interest, where $H(j\omega)$ is the transfer function of the filter.

The spectrum at the output of the filter is then $fS(f)$, where $S(f)$ is the spectrum of the input process. If only a time-limited version of the random process is available, then the spectrum at the filter input is an approximation to $S(f)$. The spectrum at the output is therefore an

approximation to $fS(f)$, here called $\widehat{fS(f)}$. Ciciora assumes the input normalized to unity power, and his estimate is

$$\hat{f} = \int_0^\infty \widehat{fS(f)}\, df = \lim_{T\to\infty} \frac{1}{2\pi T} \int_0^T |v_{BT}(t)|^2 dt \qquad (2.6)$$

where v_{BT} is the output of the specialized filter resulting from a time-limited input. After squaring, $v_{BT}(t)$ is passed through an Average-Extraction Filter (A.E.F.), which ideally is equivalent to averaging in time from zero to infinity, as shown in (2.6) above. In practice, of course, the A.E.F. has non-zero bandwidth.

Ciciora assumes the input normalized to unity power, and his device does not contain a divider. Instead of normalizing the input to unity power, however, one can divide the output of the A.E.F. by a local estimate of the input power. Although this necessitates using components of larger dynamic range throughout the system, it will be shown in Chapter IV that this division greatly reduces the variance of the estimate. Since the power in the time-limited input $v_A(t)$ is

$$\frac{1}{T}\int_0^T v_A^2(t)dt,$$

Ciciora's estimator becomes

$$2\pi\hat{f} = \frac{\int_0^{\infty} (v_{BT}(t))^2 dt}{\int_0^{T} (v_A^2(t)) dt} \tag{2.7}$$

when the divider is appended. For real-time estimates, of course, the upper limit of the numerator integral must be reduced. The effect of this reduction is discussed in Chapter IV.

A block diagram of Ciciora's device is shown in Fig. 2. In implementing this estimator, the chief difficulty is the construction of a filter for which $|H(j\omega)|^2$ approximates $|\omega|$ over the frequency range of interest. Ciciora makes the necessary frequency range narrow by means of a frequency-tracking loop which heterodynes the input signal into the range over which the approximation to $|\omega|$ is good, but this introduces additional complexity.

In summary, classical methods of estimating average frequency involve estimating $S(f)$ and then obtaining $\hat{f}$ from (2.1). Ciciora obtains an estimate of $fS(f)$ by means of a specialized filter; Denenberg derives an estimator (2.4) in terms of the two outputs of a quadrature detector, α and β.

In Chapter III, a new estimator will be introduced, and in Chapter IV, the different estimators will be compared.

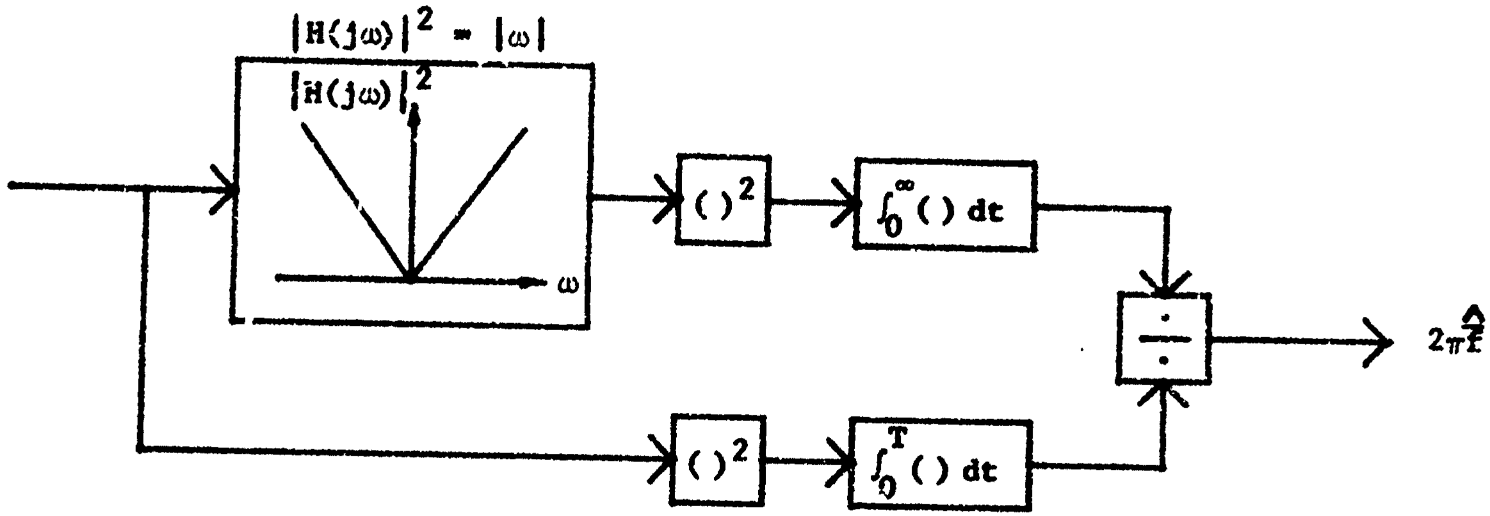

Fig. 2. Block Diagram of Ciciora's Estimator, with Divider

CHAPTER III

PROPOSED NEW ESTIMATOR

In the previous chapter, it was pointed out that there are many different ways to estimate $\bar{f}$. This is true because there are many different expressions for $\bar{f}$, all equivalent to

$$\bar{f} = \frac{\int_0^\infty f S(f)\, df}{\int_0^\infty S(f)\, df}, \tag{3.1}$$

and each expression gives rise to a different estimator.

In this chapter, it will be shown how different expressions for $\bar{f}$ lead to the different estimators already mentioned. In addition, a proposed estimator will be obtained from a new expression for $\bar{f}$. In the subsequent chapters, these different estimators will be analyzed and their relative merits considered.

The different expressions for $\bar{f}$ and $\hat{\bar{f}}$ are shown systematically in Fig. 3. It will be shown in this chapter that all the expressions for $\bar{f}$ are equivalent to each other. Therefore, the corresponding <u>estimates</u> for $\bar{f}$ all approach each other as the integrating time T approaches infinity. Of course, the relative merits of the different estimators under <u>finite</u> time is of primary concern.

First, the expressions on the frequency-domain side of Fig. 3 will be derived.

In equation (3.1), the definition for $\bar{f}$, substituting an estimate for S(f) results in an estimate of $\bar{f}$ as shown in Fig. 3, expression B.

$$\hat{\bar{f}} = \frac{\int_0^\infty f \hat{S}(f)\, df}{\int_0^\infty \hat{S}(f)\, df} \tag{3.2}$$

As pointed out in the previous chapter, if the periodogram estimate is used for S(f), Donenberg's expression C is obtained.

$$\hat{\bar{f}} = \frac{1}{2\pi} \frac{\int_0^T (\alpha\dot{\beta} - \beta\dot{\alpha})dt}{\int_0^T (\alpha^2 + \beta^2)dt} \tag{3.3}$$

If in the definition for $\bar{f}$, fS(f) is called $S_{BB}(f)$, expression D is obtained.

$$\bar{f} = \frac{\int_0^\infty S_{BB}(f)df}{\int_0^\infty S(f)\, df} \tag{3.4}$$

$S_{BB}(f)$ denotes a frequency-weighted spectrum, which Ciciora obtains by means of a specialized filter. If $v_B(t)$ is the time-domain signal corresponding to $S_{BB}(f)$, then, by Parceval's Theorem,

Frequency Domain	Time Domain
A. $\bar{f} = \dfrac{\int_0^\infty f S(f)\,df}{\int_0^\infty S(f)\,df}$ (Definition)	G. $\bar{f} = \dfrac{1}{2\pi}\dfrac{R_{A\dot{X}}(0) - R_{X\dot{A}}(0)}{R_{AA}(0) + R_{XX}(0)}$
B. $\hat{\bar{f}} = \dfrac{\int_0^\infty f\hat{S}(f)\,df}{\int_0^\infty \hat{S}(f)\,df}$	H. $\hat{\bar{f}} = \dfrac{1}{2\pi}\dfrac{\hat{R}_{A\dot{X}}(0) - \hat{R}_{X\dot{A}}(0)}{\hat{R}_{AA}(0) + \hat{R}_{XX}(0)}$ (equivalent to Denenberg's estimator).
C. $= \dfrac{1}{2\pi}\dfrac{\int_0^T (\alpha\dot{\beta} - \beta\dot{\alpha})\,dt}{\int_0^T (\alpha^2 + \beta^2)\,dt}$ if $\hat{S}(f)$ is the periodogram (Denenberg).	J. $\bar{f} = \dfrac{1}{2\pi}\dfrac{R_{A\dot{X}}(0)}{R_{AA}(0)}$
D. $\bar{f} = \dfrac{\int_0^\infty S_{BB}(f)\,df}{\int_0^\infty S(f)\,df}$ where $S_{BB}(f) = fS(f)$.	K. $\hat{\bar{f}} = \dfrac{1}{2\pi}\dfrac{\hat{R}_{A\dot{X}}(0)}{\hat{R}_{AA}(0)}$
E. $\hat{\bar{f}} = \dfrac{\int_0^\infty \hat{S}_{BB}(f)\,df}{\int_0^\infty \hat{S}(f)\,df}$	L. $\bar{f} = -\dfrac{1}{2\pi}\dfrac{R_{X\dot{A}}(0)}{R_{XX}(0)}$
F. $= \dfrac{1}{2\pi}\dfrac{\int_0^T v_{BT}^2(t)\,dt}{\int_0^T v_A^2(t)\,dt}$ where $v_{BT}(t)$ is the frequency-weighted signal [illegible]).	M. $\hat{\bar{f}} = -\dfrac{1}{2\pi}\dfrac{\hat{R}_{X\dot{A}}(0)}{\hat{R}_{XX}(0)}$ (proposed estimator)

Fig. 3. Different Expressions for $\bar{f}$ and $\hat{\bar{f}}$

$$\int_0^\infty S_{BB}(f)\,df = \frac{1}{T}\int_{-\infty}^{\infty} |v_B(t)|^2 dt \qquad (3.5)$$

Equation 3.4 is then equivalent to

$$2\pi\bar{f} = \frac{\int_{-\infty}^{\infty} v_B^2(t)\ dt}{\int_{-\infty}^{\infty} v_A^2(t)\ dt} \qquad (3.6)$$

If only a time-limited version of $v_A(t)$ is available, the denominator becomes

$$\int_0^T v_A^2(t)\ dt.$$

The result of passing this time-limited signal through Ciciora's filter is here called $v_{BT}(t)$. In general, $v_{BT}(t)$ need not be time-limited. Equation (3.6) then becomes expression $\bar{f}$ in Fig. 3.

$$2\pi\hat{f} = \frac{\int_{-\infty}^{\infty} v_{BT}^2(t)\ dt}{\int_0^T v_A^2(t)\ dt} \qquad (3.7)$$

By Parceval's Theorem, this would obviously be equivalent to (3.4) if T were infinite. Since T is finite, (3.7) is instead equivalent to E.

$$\hat{f} = \frac{\int_0^\infty \hat{S}_{BB}(t)\ df}{\int_0^\infty \hat{S}(f)\ df} \qquad (3.8)$$

All of the expressions on the frequency-domain side of Fig. 3 have now been derived. In order to derive the time-domain expressions, it is necessary to digress briefly to introduce the Hilbert Transform.

A discussion of the Hilbert Transform and analytic signal appears in Appendix A. Let $\check{v}_A(t)$ be the Hilbert Transform of $v_A(t)$, and let $z(t) = v_A(t) + j\check{v}_A(t)$ be the analytic signal associated with $v_A(t)$. If $S_{ZZ}(f)$ is the power spectral density of $z(t)$, then $S_{ZZ}(f) = 0$ when $f < 0$ and $S_{ZZ}(f) = 4S(f)$ when $f > 0$. (See Appendix A.) Therefore

$$\bar{f} = \frac{\int_{-\infty}^{\infty} f S_{ZZ}(f)\ df}{\int_{-\infty}^{\infty} S_{ZZ}(f)\ df} \qquad (3.9)$$

That is, the limits of integration in (3.1) can be changed to the entire two-sided frequency domain if S(f) is replaced with $S_{ZZ}(f)$. This change in the limits of integration will make possible the derivation of the time-domain expressions.

The autocorrelation function of the analytic signal of $v_A(t)$ can be written in terms of $S_{ZZ}(f)$ by

$$R_{ZZ}(\tau) = \int_{-\infty}^{\infty} S_{ZZ}(f)\, e^{j\omega\tau}\, df \tag{3.10}$$

Substituting $\tau = 0$ gives

$$R_{ZZ}(0) = \int_{-\infty}^{\infty} S_{ZZ}(f)\, df. \tag{3.11}$$

Differentiating (3.10) with respect to τ and substituting $\omega = 2\pi f$ gives

$$\dot{R}_{ZZ}(\tau) = j2\pi \int_{-\infty}^{\infty} f S_{ZZ}(f)\, e^{j\omega\tau}\, df. \tag{3.12}$$

Substituting $\tau = 0$ and multiplying by $-j/2\pi$ gives

$$\frac{-j}{2\pi}\,\dot{R}_{ZZ}(0) = \int_{-\infty}^{\infty} f S_{ZZ}(f)\, df. \tag{3.13}$$

Comparing (3.9) with (3.11) and (3.13) gives

$$\bar{f} = \frac{-j}{2\pi}\,\frac{\dot{R}_{ZZ}(0)}{R_{ZZ}(0)}\,. \tag{3.14}$$

By definition of the autocorrelation function of a complex process

$$R_{ZZ}(\tau) = E\left[z(t)z^{*}(t+\tau)\right] \tag{3.15}$$

where the asterisk (*) denotes the complex conjugate. Hence

$$R_{ZZ}(\tau) = E\Big[\left(v_A(t) + j\check{v}_A(t)\right) \cdot \left(v_A(t+\tau) - j\check{v}_A(t+\tau)\right)\Big]. \tag{3.16}$$

Carrying out the multiplication and making use of the distributive property of the expected value of a sum gives

$$R_{ZZ}(\tau) = E\left[v_A(t)v_A(t+\tau)\right] + E\left[\check{v}_A(t)\check{v}_A(t+\tau)\right] + jE\left[\check{v}_A(t)v_A(t+\tau)\right] - jE\left[v_A(t)\check{v}_A(t+\tau)\right] \tag{3.17}$$

or

$$R_{ZZ}(\tau) = R_{AA}(\tau) + R_{\check{A}\check{A}}(\tau) + jR_{\check{A}A}(\tau) - jR_{A\check{A}}(\tau). \tag{3.18}$$

It can be shown[9] that the last two terms in the right-hand side are zero for $\tau = 0$. Therefore

$$R_{ZZ}(0) = R_{AA}(0) + R_{\check{A}\check{A}}(0). \tag{3.19}$$

It can also be shown[9] that

$$\dot{R}_{\check{A}A}(\tau) = -R_{\check{A}\dot{A}}(\tau) \tag{3.20}$$

and

$$\dot{R}_{A\check{A}}(\tau) = -R_{A\dot{\check{A}}}(\tau). \tag{3.21}$$

Therefore, differentiating (3.18) with respect to τ gives

$$\dot{R}_{ZZ}(\tau) = \dot{R}_{AA}(\tau) + \dot{R}_{\check{A}\check{A}}(\tau) - jR_{\check{A}\dot{A}}(\tau) + jR_{A\dot{\check{A}}}(\tau). \tag{3.22}$$

Since the autocorrelation function of a real random process is an even, differentiable function of τ,

$$\dot{R}_{AA}(0) = \dot{R}_{\check{A}\check{A}}(0) = 0. \tag{3.23}$$

Therefore, substituting $\tau = 0$ in (3.22) and multiplying by $-j$ gives

$$-j\dot{R}_{ZZ}(0) = R_{A\dot{\check{A}}}(0) - R_{\check{A}\dot{A}}(0). \tag{3.24}$$

Comparing (3.14) with (3.19) and (3.24) gives expression G in Fig. 3.

$$\bar{f} \approx \frac{1}{2\pi}\,\frac{R_{A\dot{\check{A}}}(0) - R_{\check{A}\dot{A}}(0)}{R_{AA}(0) + R_{\check{A}\check{A}}(0)} \tag{3.25}$$

Under the ergodic assumption, the ensemble autocorrelation function is equal to the time autocorrelation function, and

$$2\pi\bar{f} = \frac{\mathcal{R}_{A\dot{\check{A}}}(0) - \mathcal{R}_{\check{A}\dot{A}}(0)}{\mathcal{R}_{AA}(0) + \mathcal{R}_{\check{A}\check{A}}(0)} \tag{3.26}$$

or, from the definition of $\mathcal{R}$,

$$2\pi\bar{f} = \frac{\lim\limits_{T\to\infty} \frac{1}{2T}\displaystyle\int_{-T}^{T} \left[v_A(t)\dot{\check{v}}_A(t) - \check{v}_A(t)\dot{v}_A(t)\right] dt}{\lim\limits_{T\to\infty} \frac{1}{2T}\displaystyle\int_{-T}^{T} \left[v_A^2(t) + \check{v}_A^2(t)\right] dt} \tag{3.27}$$

If $v_A(t)$ is available only for $0 < t < T$, then $\dot{v}_A(t)$ is available for the same time period. Suppose that $\check{v}_A(t)$ were also available for $0 < t < T$. Then a possible estimate for $\bar{f}$ can be given by

$$\hat{\bar{f}} = \frac{1}{2\pi}\,\frac{\displaystyle\int_0^T \left[v_A(t)\dot{\check{v}}_A(t) - \check{v}_A(t)\dot{v}_A(t)\right] dt}{\displaystyle\int_0^T \left[v_A^2(t) + \check{v}_A^2(t)\right] dt} \tag{3.28}$$

If an entire ensemble of sample functions were available, then (3.28) would be equal to (3.25). Since only one sample function is available, the autocorrelation functions and cross-correlation functions in (3.25) are only approximated. Therefore (3.28) above is equivalent to expression H in Fig. 3.

$$\hat{\bar{f}} = \frac{1}{2\pi}\,\frac{\hat{R}_{A\dot{\check{A}}}(0) - \hat{R}_{\check{A}\dot{A}}(0)}{\hat{R}_{AA}(0) + \hat{R}_{\check{A}\check{A}}(0)} \tag{3.29}$$

When a quadrature detector is applied to the received signal, the two detector outputs differ by a constant ninety degrees. Hence for real input signals, one output is the Hilbert Transform of the other. If the two outputs are labeled α and β such that β is the Hilbert Transform of α, then (3.29) can be rewritten in terms of the detector outputs by substituting α for $v_A(t)$ and β for $\check{v}_A(t)$. Then

$$\hat{\bar{f}} = \frac{1}{2\pi}\,\frac{\displaystyle\int_0^T (\alpha\dot{\beta} - \beta\dot{\alpha})\, dt}{\displaystyle\int_0^T (\alpha^2 + \beta^2)\, dt} \tag{3.30}$$

This is Denenberg's estimator C. Denenberg derived his estimator from frequency-domain expression B; it is now seen that his estimator is also derivable from time-domain expression G. This new approach will presently lead to a different estimator.

It can be easily shown[8] that

$$R_{ZZ}(\tau) = 2\left[R_{AA}(\tau) + jR_{\check{A}A}(\tau)\right] \tag{3.31}$$

Substituting $\tau = 0$ gives

$$R_{ZZ}(0) = 2\left[R_{AA}(0) + jR_{\check{A}A}(0)\right]. \tag{3.32}$$

Since[9] $R_{\check{A}A}(0) = 0$,

$$R_{ZZ}(0) = 2R_{AA}(0) = 2R_{\check{A}\check{A}}(0). \tag{3.33}$$

This result states that the power in the analytic signal is twice that of the process from which the analytic signal is constructed. This is obvious from the definition of the analytic signal, $z(t) = v_A(t) + j\check{v}_A(t)$, as well as from the result (A.11) in Appendix A.

Differentiating (3.31) with respect to τ and using (3.20) gives

$$\dot{R}_{ZZ}(\tau) = 2\left[\dot{R}_{AA}(\tau) - jR_{\check{A}\dot{A}}(\tau)\right] . \qquad (3.34)$$

Substituting $\tau = 0$ and using (3.23) gives

$$\dot{R}_{ZZ}(0) = -j2R_{\check{A}\dot{A}}(0) \qquad (3.35)$$

Comparing (3.14) with (3.33) and (3.35) gives expression L.

$$\bar{f} = \frac{j\,j2R_{\check{A}\dot{A}}(0)}{2\pi 2R_{\check{A}\check{A}}(0)} = \frac{-R_{\check{A}\dot{A}}(0)}{2\pi R_{\check{A}\check{A}}(0)} . \qquad (3.36)$$

A derivation exactly parallel with that just given above results in expression J.

$$\bar{f} = \frac{1}{2\pi}\frac{R_{A\dot{\check{A}}}(0)}{R_{AA}(0)} . \qquad (3.37)$$

Equations (3.36) and (3.37) lead to the obvious estimators M and K respectively.

$$\hat{\bar{f}} = \frac{-1}{2\pi}\frac{\hat{R}_{\check{A}\dot{A}}(0)}{\hat{R}_{\check{A}\check{A}}(0)} = \frac{-1}{2\pi}\frac{\int_0^T \beta\dot{\alpha}\,dt}{\int_0^T \beta^2\,dt} \qquad (3.38)$$

and

$$\hat{\bar{f}} = \frac{1}{2\pi}\frac{\hat{R}_{A\dot{\check{A}}}(0)}{\hat{R}_{AA}(0)} = \frac{1}{2\pi}\frac{\int_0^T \alpha\dot{\beta}\,dt}{\int_0^T \alpha^2\,dt} . \qquad (3.39)$$

It is obvious that (3.36) and (3.37) each contain half the terms of Denenberg's estimator (3.30). If, in expression (3.30), T is allowed to approach infinity, the two parts of the numerator are equal and the two parts of the denominator are equal. That is, the power in α, which is

$$\lim_{T\to\infty} \frac{1}{2T}\int_{-T}^{T} \alpha^2\,dt,$$

equals the power in β, and the average value of $\alpha\dot{\beta}$ equals that of $-\beta\dot{\alpha}$. Thus (3.38) and (3.39) are equivalent to (3.30) for infinite T. The question arises whether the simpler expressions are equivalent to (3.30) for <u>finite</u> T. Testing a simple example such as a sine-wave random process having sample functions given by $v_A^k(t) = \sin(\omega t + \phi_k)$, where ϕ is uniformly distributed over the interval from zero to 2π, reveals that the answer is negative. This leads to the question of whether, under finite T, the simpler expressions (3.38) and (3.39) are as good as Denenberg's estimator (3.30).

In order to answer this question, a probabilistic analysis of all the estimators of Fig. 3 is attempted.

CHAPTER IV

PARTIAL PROBABILISTIC ANALYSIS

In this chapter, the different estimators are statistically analyzed as much as possible for two reasons. First, it is desired to compare the estimators in order to learn which one has the best signal-to-noise ratio, and how much the devices differ in this regard. Second, in order to build any of the devices, it is desirable to know the bandwidth and dynamic range of the signal at each point in the system. This enables the builder to specify suitable components for construction.

A block diagram of Ciciora's estimator with a divider (equation (2.7)), is shown in Fig. 4. Each point in the system has been labeled with a capital letter for reference. For generality, the integrators have been shown as low-pass filters. This point will be discussed in detail later. For analytic simplicity, the specialized filter is assumed to obey $|H(j\omega)|^2 = |\omega|$ over the entire frequency domain.

Denenberg's estimator (2.4) is shown in Fig. 5. Although the diagram shows signal H derived from signal A by means of a Hilbert Transform network, in practice, signals A and H are simultaneously obtained by quadrature detection of the received signal. However, for real received signals, one quadrature detector output is the Hilbert transform of the other, there being a constant ninety-degree phase difference between the two outputs. Therefore, the Hilbert transform network shown is equivalent to the quadrature detector

used. As in Fig. 4, the integrators are shown as low-pass filters.

The estimators (3.38) and (3.39) have the same structure, since substituting $\beta = \hat{\alpha}$ for α in (3.38) results in (3.39), and β has the same power spectral density as α. Arbitrarily, (3.38) is chosen as the proposed estimator, and a block diagram is shown in Fig. 6. As in Fig. 5, a Hilbert transform network is shown in place of the quadrature detector, and the integrators are shown as low-pass filters.

Expressions will now be obtained for the autocorrelation function and power spectral density at every point in each system up to the output divider. The divider will be discussed in the next chapter.

Consider Fig. 4. Let $R_{AA}(\tau)$ be the autocorrelation function of the input process, and $S_{AA}(f)$ be its power spectral density. Then

$$R_{AA}(\tau) = \int_{-\infty}^{\infty} S_{AA}(f) e^{j\omega\tau} df \ . \tag{4.1}$$

The power spectral density at the output of Ciciora's specialized filter is given in terms of the input spectrum by

$$S_{BB}(f) = |\omega| S_{AA}(f) \ . \tag{4.2}$$

Hence,

$$R_{BB}(\tau) = \int_{-\infty}^{\infty} |\omega| S_{AA}(f) e^{j\omega\tau} df \ . \tag{4.3}$$

It is desired to find $R_{BB}(\tau)$ in terms of $R_{AA}(\tau)$.

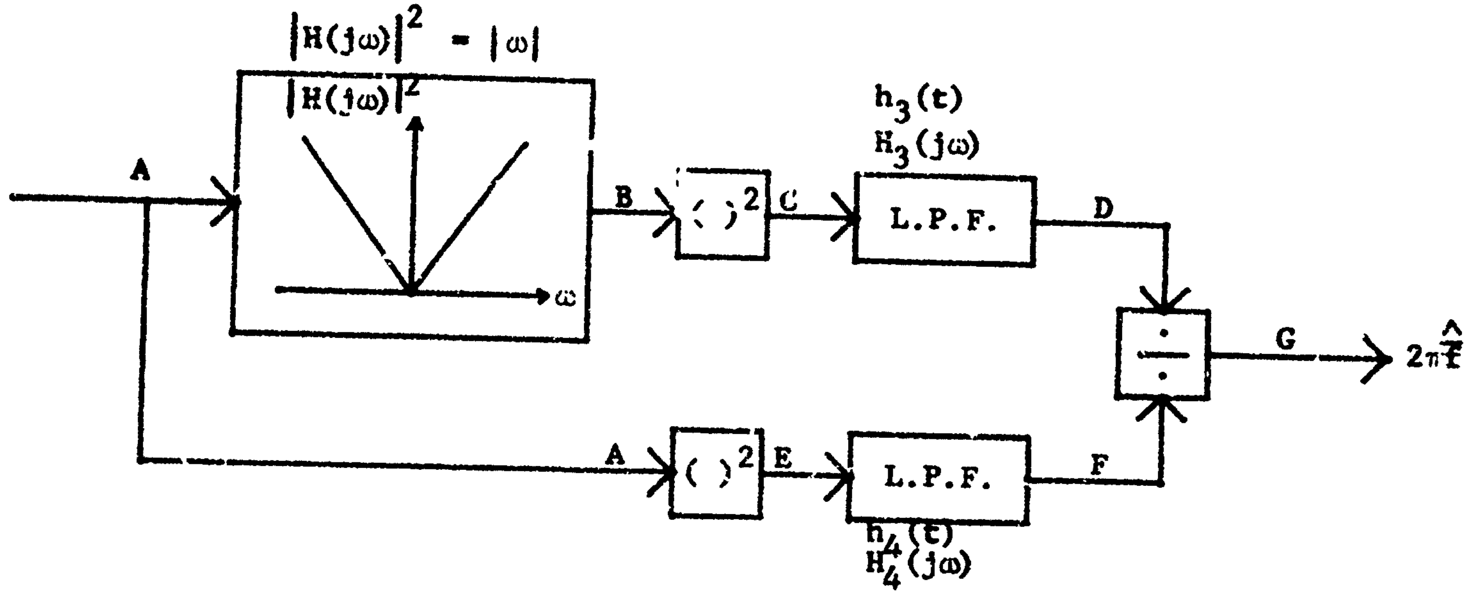

Fig. 4. Ciciora's Estimator with Divider

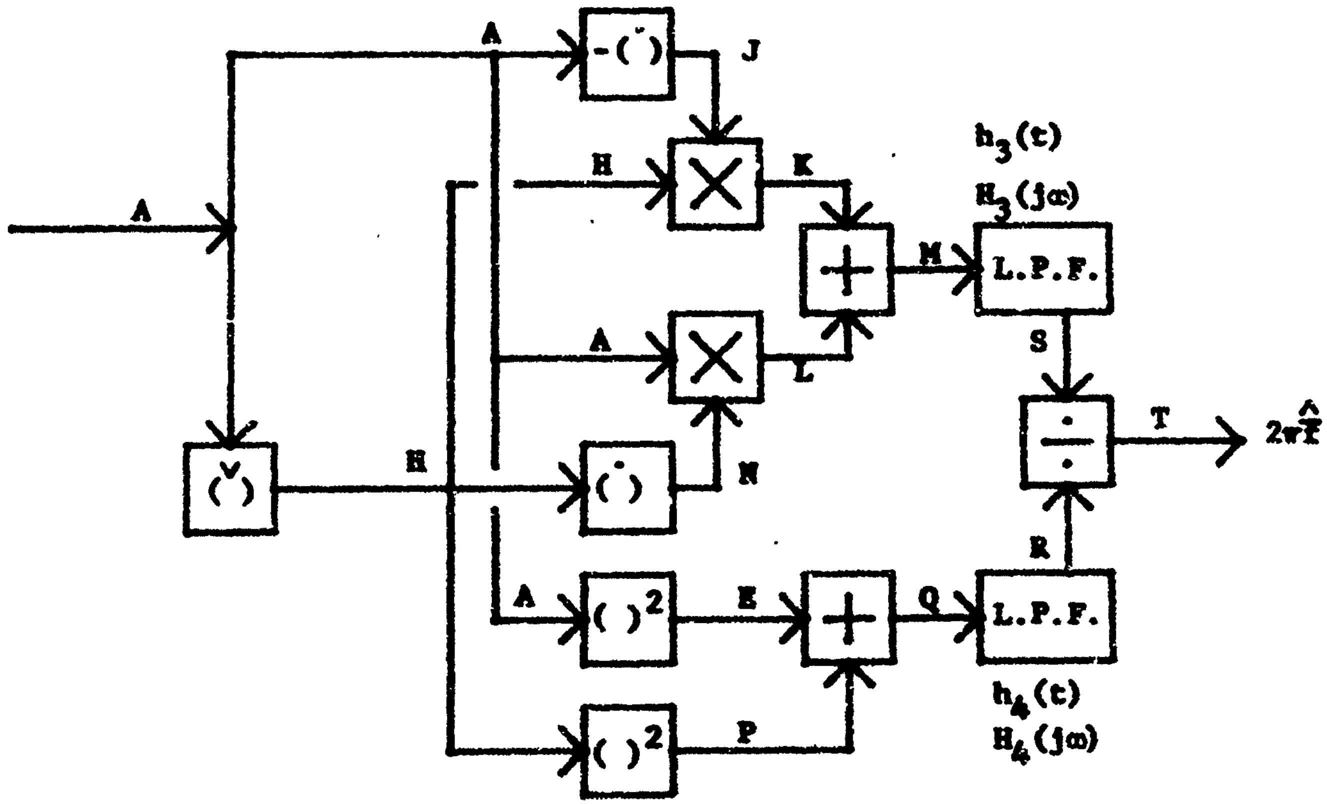

Fig. 5. Danenberg's Estimator

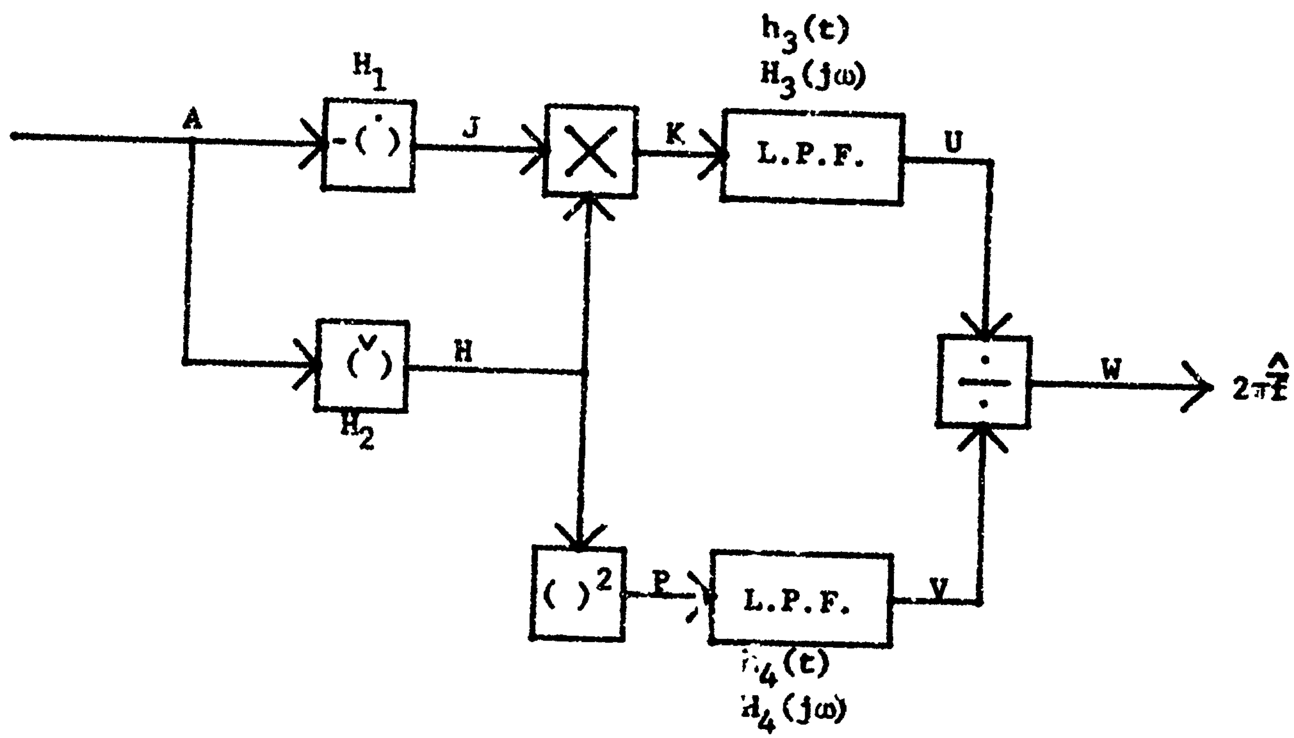

Fig. 6. Proposed Estimator

Differentiating (4.1) with respect to τ gives

$$\dot{R}_{AA}(\tau) = j\int_{-\infty}^{\infty} \omega S_{AA}(f) e^{j\omega\tau} df \ . \tag{4.4}$$

Writing this expression as the sum of two integrals gives

$$\dot{R}_{AA}(\tau) = j\int_{-\infty}^{0} \omega S_{AA}(f) e^{j\omega\tau} df + j\int_{0}^{\infty} \omega S_{AA}(f) e^{j\omega\tau} df \ . \tag{4.5}$$

In Appendix A, it is shown that the Hilbert Transform multiplies by j in the negative frequency domain and by -j in the positive frequency domain. Taking the Hilbert Transform of (4.5) therefore gives

$$\hat{\dot{R}}_{AA}(\tau) = -\int_{-\infty}^{0} \omega S_{AA}(f) e^{j\omega\tau} df + \int_{0}^{\infty} \omega S_{AA}(f) e^{j\omega\tau} df \tag{4.6}$$

or

$$\hat{\dot{R}}_{AA}(\tau) = \int_{-\infty}^{\infty} |\omega| S_{AA}(f) e^{j\omega\tau} df \ . \tag{4.7}$$

Comparing (4.3) with (4.7) gives

$$R_{BB}(\tau) = \hat{\dot{R}}_{AA}(\tau) \ . \tag{4.8}$$

Thus, the autocorrelation function at point B in the system is the Hilbert Transform of the derivative of the input autocorrelation function. The spectrum at that point is given by (4.2).

If the input is a real, gaussian random process of zero mean, then so is the signal at B, since the specialized filter is a linear, time-invariant network. In this case, it can be shown[3] that the following equation holds for the

squarer B-C:

$$R_{CC}(\tau) = R_{BB}^2(0) + 2R_{BB}^2(\tau) \tag{4.9}$$

and, similarly, for the squarer A-E,

$$R_{EE}(\tau) = R_{AA}^2(0) + 2R_{AA}^2(\tau) \ . \tag{4.10}$$

Substituting (4.8) in (4.9) gives

$$R_{CC}(\tau) = \hat{\dot{R}}_{AA}^2(0) + 2\hat{\dot{R}}_{AA}^2(\tau) \ . \tag{4.11}$$

The first term in the right-hand side is a constant. The above expression can, therefore, be rewritten in terms of the power spectral density if (4.7) is used:

$$S_{CC}(\omega) = 2\pi \hat{\dot{R}}_{AA}^2(0)\, \delta(\omega) + 2\left(|\omega| S_{AA}(\omega)\right) * \left(|\omega| S_{AA}(\omega)\right) \tag{4.12}$$

where $\delta(\omega)$ is the Dirac delta function, or unit impulse, and the asterisk (*) represents convolution.

Similarly, (4.10) can be rewritten as

$$S_{EE}(\omega) = 2\pi R_{AA}^2(0)\, \delta(\omega) + 2S_{AA}(\omega) * S_{AA}(\omega) \ . \tag{4.13}$$

If C-D and E-F are "integrate-and-dump" devices, then the "signals" at D and F consist of single numbers rather than time-varying voltages. If, however, C-D and E-F are considered to be low-pass filters, as shown in Fig. 4, then expressions can be obtained for the autocorrelation function and power spectral density at D and F.

If $H_3(j\omega)$ is the transfer function of low-pass filter C-D, then

$$S_{DD}(\omega) = \left|H_3(j\omega)\right|^2 S_{CC}(\omega) \tag{4.14}$$

and

$$R_{DD}(\tau) = \frac{1}{2\pi}\int_{-\infty}^{\infty} S_{DD}(f)e^{j\omega\tau}df$$

$$= \int_{-\infty}^{\infty}\int_{-\infty}^{\infty} h_3(t_1)h_3(t_2)R_{CC}(t_2+\tau-t_1)dt_1dt_2 \ . \qquad (4.15)$$

Similarly, if $H_4(j\omega)$ is the transfer function of filter E-F, then

$$S_{FF}(\omega) = \left|H_4(j\omega)\right|^2 S_{EE}(\omega) \qquad (4.16)$$

and

$$R_{FF}(\omega) = \frac{1}{2\pi}\int_{-\infty}^{\infty} S_{EE}(f)e^{j\omega\tau}df$$

$$= \int_{-\infty}^{\infty}\int_{-\infty}^{\infty} h_4(t_1)h_4(t_2)R_{EE}(t_2+\tau-t_1)dt_1dt_2 \ . \qquad (4.17)$$

In Denenberg's device, Fig. 5, Hilbert transform network A-H is an all-pass filter with $\left|H(j\omega)\right|^2 = 1$. Thus,

$$S_{HH}(\omega) = S_{AA}(\omega) \ . \qquad (4.18)$$

Therefore,

$$R_{HH}(\tau) = R_{AA}(\tau) \ . \qquad (4.19)$$

For the negative differentiator A-J, $\left|H(j\omega)\right|^2 = \omega^2$. Thus,

$$S_{JJ}(\omega) = \omega^2 S_{AA}(\omega) \qquad (4.20)$$

and

$$R_{JJ}(\tau) = \int_{-\infty}^{\infty} \omega^2 S_{AA}(\omega)e^{j\omega\tau}d\tau \ . \qquad (4.21)$$

It is desired to find $R_{JJ}(\tau)$ in terms of $R_{AA}(\tau)$. Taking the

derivative of (4.4) with respect to τ gives

$$\ddot{R}_{AA}(\tau) = -\int_{-\infty}^{\infty} \omega^2 S_{AA}(\omega)e^{j\omega\tau}d\tau \ . \qquad (4.22)$$

Comparing with (4.21) gives

$$R_{JJ}(\tau) = -\ddot{R}_{AA}(\tau) \ . \qquad (4.23)$$

To find the autocorrelation function at K, assume that the signal at A is a real, gaussian random process of zero mean. Then so are the signals at H and J, because A-H and A-J are linear, time-invariant networks. In this case, the following expression for the product of four random variables can be shown[3] to hold true:

$$E\left[x_1x_2x_3x_4\right] = E\left[x_1x_2\right]E\left[x_3x_4\right] + E\left[x_1x_3\right]E\left[x_2x_4\right] + E\left[x_1x_4\right]E\left[x_2x_3\right] \qquad (4.24)$$

Let $x_1 = v_J(t)$, $x_2 = v_H(t)$, $x_3 = v_J(t+\tau)$, and $x_4 = v_H(t+\tau)$. Then

$$\begin{aligned} x_1x_2 &= v_J(t)v_H(t) = v_K(t) \\ x_3x_4 &= v_J(t+\tau)v_H(t+\tau) = v_K(t+\tau) \\ x_1x_3 &= v_J(t)v_J(t+\tau) \\ x_2x_4 &= v_H(t)v_H(t+\tau) \\ x_1x_4 &= v_J(t)v_H(t+\tau) \\ x_2x_3 &= v_H(t)v_J(t+\tau) \end{aligned} \qquad (4.25)$$

and (4.24) can be rewritten as

$$R_{KK}(\tau) = R_{JH}^2(0) + R_{JJ}(\tau)R_{HH}(\tau) + R_{JH}(\tau)R_{HJ}(\tau) \ . \qquad (4.26)$$

The autocorrelation functions in the right-hand side are known in terms of $R_{AA}(\tau)$, but the cross-correlation functions are not yet known. These can be found from the general expressions for the cross-correlation function of the outputs of two linear, time-invariant networks[11]:

$$R_{y_a y_b}(\tau) = R_{x_a y_b}(\tau) * h_a(\tau)$$
$$R_{x_a y_b}(\tau) = R_{x_a x_b}(\tau) * h_b^*(-\tau) \qquad (4.27)$$

where the x's are the inputs and the y's are the outputs of networks a and b. In this case, the impulse responses of both networks A-J and A-H are real, odd functions of time, and $h_b^*(-\tau)$ can be replaced with $-h_b(\tau)$.

In applying (4.27) to Fig. 5, let both x_a and x_b be v_a. If $y_a = v_J$ and $y_b = v_H$, an expression for $R_{JH}(\tau)$ is obtained. From (4.27)

$$R_{JH}(\tau) = R_{AH}(\tau) * h_1(\tau) = -\dot{R}_{AH}(\tau)$$
$$R_{AH}(\tau) = R_{AA}(\tau) * (-h_2(\tau)) = -\check{R}_{AA}(\tau) \qquad (4.28)$$

Thus

$$R_{JH}(\tau) = \dot{\check{R}}_{AA}(\tau) \ . \qquad (4.29)$$

If $y_a = v_H$ and $y_b = v_J$, an expression for $R_{HJ}(\tau)$ is found. From (4.25),

$$R_{HJ}(\tau) = R_{AJ}(\tau) * h_2(\tau) = \check{R}_{AJ}(\tau)$$
$$R_{AJ}(\tau) = R_{AA}(\tau) * (-h_1(\tau)) = \dot{R}_{AA}(\tau) \qquad (4.30)$$

Thus

$$R_{HJ}(\tau) = \check{\dot{R}}_{AA}(\tau) \ . \qquad (4.31)$$

Since both differentiation and the Hilbert Transform are linear operators, the right-hand sides of (4.29) and (4.31) are the same.

Substituting (4.19), (4.23), (4.29), and (4.31) in (4.26) gives

$$R_{KK}(\tau) = \check{\dot{R}}^2_{AA}(0) - R_{AA}(\tau)\ddot{R}_{AA}(\tau) + \check{\dot{R}}^2_{AA}(\tau) \qquad (4.32)$$

This can be rewritten in terms of power spectral densities if (4.7) and (4.22) are used:

$$S_{KK}(\omega) = 2\pi\check{\dot{R}}^2_{AA}(0)\delta(\omega) + S_{AA}(\omega) * \left(\omega^2 S_{AA}(\omega)\right)$$
$$+ \left(|\omega| S_{AA}(\omega)\right) * \left(|\omega| S_{AA}(\omega)\right) \ . \qquad (4.33)$$

The signal that is now at K will be obtained at L if the input is replaced with the Hilbert Transform of the input. However, such a replacement would change neither $R_{AA}(\tau)$ nor $S_{AA}(\omega)$, and $R_{KK}(\tau)$ and $S_{KK}(\omega)$ have been obtained in terms of these functions. Therefore,

$$R_{LL}(\tau) = R_{KK}(\tau) \qquad (4.34)$$

and

$$S_{LL}(\omega) = S_{KK}(\omega) \ . \qquad (4.35)$$

Since the spectrum at H is the same as the spectrum at A,

$$S_{NN}(\omega) = S_{JJ}(\omega) \qquad (4.36)$$

and

$$R_{NN}(\tau) = R_{JJ}(\tau) \ . \qquad (4.37)$$

In order to find the spectrum and autocorrelation function at point M in Fig. 5, consider the diagram in Fig. 7, which shows two means of obtaining $v_N(t) = \check{\dot{v}}_A(t)$.

In Fig. 5, $v_M(t)$ can be written

$$v_M(t) = v_A(t)\check{\dot{v}}_A(t) - \check{v}_A(t)\dot{v}_A(t) \ . \qquad (4.38)$$

In terms of the labels on Fig. 7, this is

$$v_M(t) = v_A(t)v_N(t) - v_H(t)v_X(t) \ . \qquad (4.39)$$

At time $t+\tau$, this can be written

$$v_M(t+\tau) = v_A(t+\tau)v_N(t+\tau) - v_H(t+\tau)v_X(t+\tau) \ . \qquad (4.40)$$

Multiplying (4.39) by (4.40) and taking the expected value gives

$$\begin{aligned} E\left[v_M(t)v_M(t+\tau)\right] &= E\left[v_A(t)v_A(t+\tau)v_N(t)v_N(t+\tau)\right] \\ &+ E\left[v_H(t)v_H(t+\tau)v_X(t)v_X(t+\tau)\right] \\ &- E\left[v_A(t)v_X(t+\tau)v_N(t)v_H(t+\tau)\right] \\ &- E\left[v_X(t)v_A(t+\tau)v_H(t)v_N(t+\tau)\right] \qquad (4.41) \end{aligned}$$

or, using equation (4.24),

$$\begin{aligned} E\left[v_M(t)v_M(t+\tau)\right] &= E\left[v_A(t)v_A(t+\tau)\right]E\left[v_N(t)v_N(t+\tau)\right] \\ &+ E\left[v_A(t)v_N(t)\right]E\left[v_A(t+\tau)v_N(t+\tau)\right] \\ &+ E\left[v_A(t)v_N(t+\tau)\right]E\left[v_A(t+\tau)v_N(t)\right] \\ &+ E\left[v_H(t)v_H(t+\tau)\right]E\left[v_X(t)v_X(t+\tau)\right] \\ &+ E\left[v_H(t)v_X(t)\right]E\left[v_H(t+\tau)v_X(t+\tau)\right] \end{aligned}$$

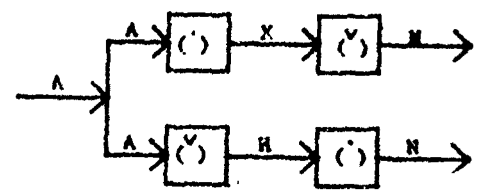

Fig. 7. Two Methods of Obtaining $v_N(t) = v_A(t)$

$$\begin{aligned} &+ E\left[v_H(t)v_X(t+\tau)\right]E\left[v_H(t+\tau)v_X(t)\right] \\ &- E\left[v_A(t)v_X(t+\tau)\right]E\left[v_N(t)v_H(t+\tau)\right] \\ &- E\left[v_A(t)v_N(t)\right]E\left[v_X(t+\tau)v_H(t+\tau)\right] \\ &- E\left[v_A(t)v_H(t+\tau)\right]E\left[v_X(t+\tau)v_N(t)\right] \\ &- E\left[v_X(t)v_A(t+\tau)\right]E\left[v_H(t)v_N(t+\tau)\right] \\ &- E\left[v_X(t)v_H(t+\tau)\right]E\left[v_A(t+\tau)v_N(t+\tau)\right] \\ &- E\left[v_X(t)v_N(t+\tau)\right]E\left[v_A(t+\tau)v_H(t)\right] \ . \qquad (4.42) \end{aligned}$$

Thus

$$\begin{aligned} R_{MM}(\tau) &= R_{AA}(\tau)R_{NN}(\tau) + R_{AN}^2(0) + R_{AN}(\tau)R_{NA}(\tau) \\ &+ R_{HH}(\tau)R_{XX}(\tau) + R_{HX}^2(0) + R_{HX}(\tau)R_{XH}(\tau) - R_{AX}(\tau)R_{NH}(\tau) \\ &- R_{AN}(0)R_{XH}(0) - R_{AH}(\tau)R_{NX}(\tau) - R_{XA}(\tau)R_{HN}(\tau) \\ &- R_{XH}(0)R_{AN}(0) - R_{XN}(\tau)R_{HA}(\tau) \ . \qquad (4.43) \end{aligned}$$

The autocorrelation functions and cross-correlation functions in (4.43) will now be expressed in terms of $R_{AA}(\tau)$. Since X-N and A-H are all-pass networks,

$$R_{NN}(\tau) = R_{XX}(\tau)$$
$$R_{HH}(\tau) = R_{AA}(\tau) \;. \tag{4.44}$$

Since the spectrum at H is the same as that at A,

$$R_{HN}(\tau) = R_{AX}(\tau)$$
$$R_{NH}(\tau) = R_{XA}(\tau) \;. \tag{4.45}$$

$R_{XN}(\tau)$, $R_{NX}(\tau)$, $R_{XH}(\tau)$, and $R_{HX}(\tau)$ can be obtained from (4.27). Therefore,

$$R_{XN}(\tau) = \check{\dot{R}}_{AA}(\tau)$$
$$R_{NX}(\tau) = -\check{\dot{R}}_{AA}(\tau)$$
$$R_{XH}(\tau) = \dot{R}_{AA}(\tau) \tag{4.46}$$
$$R_{HX}(\tau) = -\dot{R}_{AA}(\tau)$$

The autocorrelation function of a random variable is the same as the autocorrelation function of its negative. Therefore, equation (4.23) gives

$$R_{XX}(\tau) = -\ddot{R}_{AA}(\tau) . \tag{4.47}$$

From (4.28)

$$R_{AH}(\tau) = -\check{R}_{AA}(\tau) . \tag{4.48}$$

Since R_{AA} is an even function, $\check{R}_{AA}$ is odd. Therefore, $R_{AH} = -\check{R}_{AA}$ is odd, and

$$R_{HA}(\tau) = R_{AH}(-\tau) = \check{R}_{AA}(\tau) \;. \tag{4.49}$$

Since $v_X(t)$ is the negative of $v_J(t)$, equations (4.29) and (4.31) give

$$R_{XH}(\tau) = -\check{\ddot{R}}_{AA}(\tau)$$
$$R_{HX}(\tau) = -\check{\ddot{R}}_{AA}(\tau) \tag{4.50}$$

Similarly, (4.30) gives

$$R_{AX}(\tau) = -\dot{R}_{AA}(\tau) \;, \tag{4.51}$$

and, since $\dot{R}_{AA}$ is odd,

$$R_{XA}(\tau) = -R_{AX}(\tau) = \dot{R}_{AA}(\tau) \;. \tag{4.52}$$

In equation (4.43), only $R_{AN}(\tau)$ and $R_{NA}(\tau)$ must still be expressed in terms of $R_{AA}(\tau)$. In order to do this, let $h_5(t)$ be the impulse response of a single network that takes the derivative of the Hilbert Transform of its input (process A-N in Fig. 7). Then a derivation similar to that of equations (4.28) gives

$$R_{AN}(\tau) = R_{AA}(\tau) * h_5^*(-\tau) \;. \tag{4.53}$$

Since h_5 is a real, even function,

$$R_{AN}(\tau) = R_{AA}(\tau) * h_5(\tau) \tag{4.54}$$

or

$$R_{AN}(\tau) = \check{\dot{R}}_{AA}(\tau) \;. \tag{4.55}$$

Since $\check{\dot{R}}_{AA}$ is an even function,

$$R_{NA}(\tau) = R_{AN}(\tau) = \check{\dot{R}}_{AA}(\tau) \tag{4.56}$$

Substituting (4.55), (4.56), and (4.44) through (4.52) in equation (4.43) gives

$$R_{MM}(\tau) = -2R_{AA}(\tau)\ddot{R}_{AA}(\tau) + 4\check{R}^2_{AA}(0) + 2\check{R}^2_{AA}(\tau)$$

$$- 2\dot{R}^2_{AA}(\tau) - 2\check{R}_{AA}(\tau)\ddot{\check{R}}_{AA}(\tau) \qquad (4.57)$$

In order to write an expression for $S_{MM}(f)$, it is first necessary to find the spectra associated with $\dot{R}^2_{AA}(\tau)$ and $\check{R}^2_{AA}(\tau)$.

From (4.4), $\dot{R}_{AA}(\tau)$ is the autocorrelation function associated with $j\omega S_{AA}(f)$. Therefore, the spectrum corresponding to $\dot{R}^2_{AA}(\tau)$ is $j\omega S_{AA}(f) * j\omega S_{AA}(f)$ or $-\left(\omega S_{AA}(f) * \omega S_{AA}(f)\right)$. In order to find the spectrum associated with $\check{R}_{AA}(\tau)$, (4.1) is rewritten as

$$R_{AA}(\tau) = \int_{-\infty}^{0} S_{AA}(f)e^{j\omega\tau}df + \int_{0}^{\infty} S_{AA}(f)e^{j\omega\tau}df \ . \qquad (4.58)$$

Taking the Hilbert Transform with respect to τ gives

$$\check{R}_{AA}(\tau) = \int_{-\infty}^{0} jS_{AA}(f)e^{j\omega\tau}df - \int_{0}^{\infty} jS_{AA}(f)e^{j\omega\tau}df \ . \qquad (4.59)$$

Define a function $W(f)$ by

$$W(f) = 1 \quad \text{for } f \ \ 0$$
$$= -1 \quad \text{for } f \ \ 0 \ . \qquad (4.60)$$

Then

$$\check{R}_{AA}(\tau) = \int_{-\infty}^{\infty} jW(f)S_{AA}(f)e^{j\omega\tau}df \ . \qquad (4.61)$$

The spectrum of $\check{R}^2_{AA}(\tau)$ is then $\left(jW(f)S_{AA}(f)\right) * \left(jW(f)S_{AA}(f)\right)$, or $-\left(W(f)S_{AA}(f)\right) * \left(W(f)S_{AA}(f)\right)$. From (4.57), the spectrum at M is thus given by

$$S_{MM}(f) = 2S_{AA}(f) * \omega^2 S_{AA}(f) + 8\check{R}^2_{AA}(0)\delta(\omega)$$
$$+ 2\left(|\omega|S_{AA}(f)\right) * \left(|\omega|S_{AA}(f)\right) + 2\left(\omega S_{AA}(f)\right) * \left(\omega S_{AA}(f)\right)$$
$$- 2\left(\omega^2 W(\omega)S_{AA}(\omega)\right) * \left(W(\omega)S_{AA}(\omega)\right) \qquad (4.62)$$

The autocorrelation function at Q can be found by writing

$$v_Q(t) = v_A(t)v_A(t) + v_H(t)v_H(t)$$
$$v_Q(t+\tau) = v_A(t+\tau)v_A(t+\tau) + v_H(t+\tau)v_H(t+\tau) \ . \qquad (4.63)$$

Taking the expected value of the product gives

$$E\left[v_Q(t)v_Q(t+\tau)\right] = E\left[v_A(t)v_A(t)v_A(t+\tau)v_A(t+\tau)\right]$$
$$+ E\left[v_H(t)v_H(t)v_H(t+\tau)v_H(t+\tau)\right]$$
$$+ E\left[v_A(t+\tau)v_A(t+\tau)v_H(t)v_H(t)\right]$$
$$+ E\left[v_A(t)v_A(t)v_H(t+\tau)v_H(t+\tau)\right] \ . \qquad (4.64)$$

Applying (4.24) and rewriting in terms of autocorrelation and cross-correlation functions gives

$$R_{QQ}(\tau) = R^2_{AA}(0) + 2R^2_{AA}(\tau) + R^2_{HH}(0) + 2R^2_{HH}(\tau)$$
$$+ 2R_{AA}(0)R_{HH}(0) + 2R^2_{HA}(\tau) + 2R^2_{AH}(\tau) \ . \qquad (4.65)$$

Substituting (4.19), (4.28), and (4.49) in (4.65) gives

$$R_{QQ}(\tau) = 4R^2_{AA}(0) + 4R^2_{AA}(\tau) + 4\check{R}^2_{AA}(\tau) \qquad (4.66)$$

The spectrum at Q is then given by

$$S_{QQ}(\omega) = 8R^2_{AA}(0)\delta(\omega) + 4S_{AA}(f) * S_{AA}(f)$$
$$- 4\left(W(f)S_{AA}(f) * W(f)S_{AA}(f)\right) \ . \qquad (4.67)$$

Squarer H-P is the same as squarer A-E, and the spectrum at H has been shown to be the same as that at A. Therefore,

$$S_{PP}(f) = S_{EE}(f) \tag{4.68}$$

and

$$R_{PP}(\tau) = R_{EE}(\tau) \ . \tag{4.69}$$

Low-pass filters M-S and Q-R are treated exactly as C-D and E-F in Ciciora's device, and, therefore,

$$S_{SS}(\omega) = \left|H_3(j\omega)\right|^2 S_{MM}(\omega) \ , \tag{4.70}$$

$$R_{SS}(\tau) = \frac{1}{2\pi}\int_{-\infty}^{\infty} S_{SS}(f)e^{j\omega\tau}df = \int_{-\infty}^{\infty}\int_{-\infty}^{\infty} h_3(t_1)h_3(t_2)R_{MM}(t_2+\tau-t_1) \cdot dt_1dt_2 \ , \tag{4.71}$$

$$S_{RR}(\omega) = \left|H_4(j\omega)\right|^2 S_{QQ}(\omega) \ , \tag{4.72}$$

and

$$R_{RR}(\tau) = \frac{1}{2\pi}\int_{-\infty}^{\infty} S_{RR}(f)e^{j\omega\tau}df$$

$$= \int_{-\infty}^{\infty}\int_{-\infty}^{\infty} h_4(t_1)h_4(t_2)R_{QQ}(t_2+\tau-t_1)dt_1dt_2 \ . \tag{4.73}$$

In the proposed estimator, Fig. 6, points P, H, J, and K correspond exactly to similarly-labeled points in the other estimators, and thus equations (4.68), (4.69), (4.18), (4.19), (4.20), (4.21), (4.32), and (4.33) are applicable. Also, what has been said before of the low-pass filters applies here, and

$$S_{HH}(\omega) = \left|H_3(j\omega)\right|^2 S_{KK}(\omega) \ , \tag{4.74}$$

$$R_{HH}(\tau) = \frac{1}{2\pi}\int_{-\infty}^{\infty} S_{HH}(f)e^{j\omega\tau}df$$

$$= \int_{-\infty}^{\infty}\int_{-\infty}^{\infty} h_3(t_1)h_3(t_2)R_{KK}(t_2+\tau-t_1)dt_1dt_2 \ , \tag{4.75}$$

$$S_{VV}(\omega) = \left|H_4(j\omega)\right|^2 S_{PP}(\omega) \ , \tag{4.76}$$

and

$$R_{VV}(\tau) = \frac{1}{2\pi}\int_{-\infty}^{\infty} S_{VV}(f)e^{j\omega\tau}df$$

$$= \int_{-\infty}^{\infty}\int_{-\infty}^{\infty} h_4(t_1)h_4(t_2)R_{PP}(t_2+\tau-t_1)dt_1dt_2 \ . \tag{4.77}$$

The autocorrelation function and power spectral density have now been found for every point in each device, up to the output divider.

It is instructive to compare the responses of the different devices to a cosine-wave random process with sample functions $v_A^k(t) = \cos(\omega_o t+\theta_k)$, where θ is uniformly distributed over the interval from zero to 2π. For simplicity, consider first the particular case where $\theta_k = 0$. The effect of the phase θ will be considered later. If

$$v_A(t) = \cos \omega_o t \tag{4.78}$$

then, in Ciciora's device,

$$v_E(t) = \cos^2 \omega_o t \ . \tag{4.79}$$

The phase response of Ciciora's specialized filter is not specified. If it is arbitrarily assumed to have zero phase

shift at ω_o, then

$$v_B(t) = \sqrt{\omega_o}\cos\omega_o t \qquad (4.80)$$

and

$$v_C(t) = \omega_o\cos^2\omega_o t \qquad (4.81)$$

If the low-pass filters are integrators,

$$2\pi\hat{f} = \frac{\int_0^T \omega_o\cos^2\omega_o t\,dt}{\int_0^T \cos^2\omega_o t\,dt} = \omega_o \qquad (4.82)$$

and Ciciora's estimator is perfect in this case.

If, however, the specialized filter is assumed to have a ninety-degree phase shift at ω_o, then

$$v_B(t) = \sqrt{\omega_o}\sin\omega_o t\ , \qquad (4.83)$$

$$v_C(t) = \omega_o\sin^2\omega_o t\ , \qquad (4.84)$$

and

$$2\pi\hat{f} = \frac{\int_0^T \omega_o\sin^2\omega_o t\,dt}{\int_0^T \cos^2\omega_o t\,dt}\ . \qquad (4.85)$$

In this case, Ciciora's estimator is not perfect, even for an input signal of zero bandwidth. The integrals of (4.82) are shown graphically in Fig. 8. Although the ratio of area A_1 to A_2 is ω_o, shaded areas A_3 and A_4 do not have this ratio. This gives rise to an error in the estimate. If the

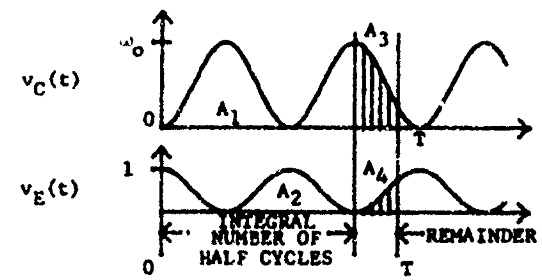

Fig. 8. Signals at C and E in Ciciora's Estimator, for Single-Frequency Input

integrating time T happens to cover an integral number of half-cycles of $v_C(t)$, however, then A_3 and A_4 are zero and the estimator is perfect in that case. Also, if the integrating time is long enough to include many cycles of $v_C(t)$, then A_3 and A_4 are negligible compared to A_1 and A_2, and the estimator is nearly perfect. If zero phase shift is assumed for filter A-B, the estimator is perfect for a single-frequency input regardless of the integrating time.

It has been shown that, for $v_A(t) = \cos\omega_o t$, the quality of Ciciora's estimator depends upon the phase shift of network A-B. This conclusion remains true when any phase ϕ_k is added to $\omega_o t$. It will now be shown that, for this simple input process having sample functions $v_A^k(t) = \cos(\omega_o t + \phi_k)$, ($\phi$ uniformly distributed over the interval from

zero to 2π), the other two estimators are perfect. Again, consider first the case where $\phi_k = 0$; the conclusion will be the same for a random ϕ. Assume $\omega_o > 0$. In Denenberg's device

$$v_H(t) = \sin \omega_o t \ , \tag{4.86}$$

$$v_J(t) = \omega_o \sin \omega_o t \tag{4.87}$$

$$v_K(t) = \omega_o \sin^2 \omega_o t \tag{4.88}$$

$$v_N(t) = \omega_o \cos \omega_o t \tag{4.89}$$

$$v_L(t) = \omega_o \cos^2 \omega_o t \tag{4.90}$$

$$v_M(t) = \omega_o \tag{4.91}$$

$$v_P(t) = \sin^2 \omega_o t \tag{4.92}$$

$$v_E(t) = \cos^2 \omega_o t \tag{4.93}$$

$$v_Q(t) = 1 \tag{4.94}$$

and

$$2\pi\hat{f} = \frac{\int_0^T \omega_o dt}{\int_0^T 1 \, dt} = \omega_o \ , \tag{4.95}$$

a perfect estimator.

In the proposed device, equations (4.86), (4.87), (4.88), and (4.92) above apply. Therefore,

$$2\pi\hat{f} = \frac{\int_0^T \omega_o \sin^2 \omega_o t \, dt}{\int_0^T \sin^2 \omega_o t \, dt} = \omega_o \ , \tag{4.96}$$

again a perfect estimator.

Consider now the case where $v_A^k(t) = \cos(\omega_o t + \phi_{ok}) + \cos(\omega_1 t + \phi_{1k})$, where ϕ_{ok} and ϕ_{1k} are uniformly distributed over the interval from zero to 2π and statistically independent. Consider first the particular case where

$$v_A(t) = \cos \omega_o t + \cos \omega_1 t \ , \tag{4.97}$$

In Ciciora's device, if the specialized filter has no phase shift,

$$v_B(t) = \sqrt{\omega_o} \cos \omega_o t + \sqrt{\omega_1} \cos \omega_1 t \ , \tag{4.98}$$

$$v_C(t) = \omega_o \cos^2 \omega_o t + \omega_1 \cos^2 \omega_1 t + 2\sqrt{\omega_o \omega_1} \cos \omega_o t \cos \omega_1 t \ , \tag{4.99}$$

$$v_E(t) = \cos^2 \omega_o t + \cos^2 \omega_1 t + 2 \cos \omega_o t \cos \omega_1 t \ , \tag{4.100}$$

and

$$2\pi\hat{f} = \frac{\int_0^T (\omega_o \cos^2 \omega_o t + \omega_1 \cos^2 \omega_1 t + 2\sqrt{\omega_o \omega_1} \cos \omega_o t \cos \omega_1 t) dt}{\int_0^T (\cos^2 \omega_o t + \cos^2 \omega_1 t + 2 \cos \omega_o t \cos \omega_1 t) dt} \tag{4.101}$$

In Denenberg's device, under the assumption $\omega_o > 0$ and $\omega_1 > 0$,

$$v_H(t) = \sin \omega_o t + \sin \omega_1 t \ , \tag{4.102}$$

$$v_J(t) = \omega_o \sin \omega_o t + \omega_1 \sin \omega_1 t \ , \tag{4.103}$$

$$v_K(t) = \omega_o \sin^2 \omega_o t + \omega_1 \sin^2 \omega_1 t + (\omega_o+\omega_1) \sin \omega_o t \sin \omega_1 t \quad , \tag{4.104}$$

$$v_N(t) = \omega_o \cos \omega_o t + \omega_1 \cos \omega_1 t \tag{4.105}$$

$$v_L(t) = \omega_o \cos^2 \omega_o t + \omega_1 \cos^2 \omega_1 t + (\omega_o+\omega_1) \cos \omega_o t \cos \omega_1 t \quad , \tag{4.106}$$

$$v_M(t) = \omega_o + \omega_1 + (\omega_o+\omega_1) \cos(\omega_o-\omega_1) t \quad , \tag{4.107}$$

$$v_P(t) = \sin^2 \omega_o t + \sin^2 \omega_1 t + 2 \sin \omega_o t \sin \omega_1 t \quad , \tag{4.108}$$

$$v_Q(t) = 2 + 2 \cos(\omega_o - \omega_1) t \quad , \tag{4.109}$$

and

$$2\pi\hat{f} = \frac{\int_0^T (\omega_o+\omega_1+(\omega_o+\omega_1)\cos(\omega_o-\omega_1)t)dt}{\int_0^T (2+2\cos(\omega_o-\omega_1)t)dt} = \frac{\omega_o+\omega_1}{2} \tag{4.110}$$

In the proposed device,

$$2\pi\hat{f} = \frac{\int_0^T (\omega_o \sin^2\omega_o t+\omega_1 \sin^2\omega_1 t+(\omega_o+\omega_1)\sin \omega_o t \sin \omega_1 t)dt}{\int_0^T (\sin^2\omega_o t + \sin^2\omega_1 t + 2 \sin \omega_o t \sin \omega_1 t)dt} \quad . \tag{4.111}$$

In order to facilitate comparison, equations (4.101) and (4.111) are rewritten using the trigonometric identities for the product of two sines and two cosines.

In Ciciora's device, from (4.101),

$$2\pi\hat{f} = \frac{\int_0^T (\omega_o\cos^2\omega_o t+\omega_1\cos^2\omega_1 t+\sqrt{\omega_o\omega_1}\cos(\omega_o-\omega_1)t+\sqrt{\omega_o\omega_1}\cos(\omega_o+\omega_1)t)dt}{\int_0^T (\cos^2\omega_o t + \cos^2\omega_1 t + \cos(\omega_o-\omega_1)t + \cos(\omega_o+\omega_1)t)dt} \tag{4.112}$$

In the proposed device, from (4.111),

$$2\pi\hat{f} = \frac{\int_0^T \left(\omega_o\sin^2\omega_o t+\omega_1\sin^2\omega_1 t+\frac{\omega_o+\omega_1}{2}\cos(\omega_o-\omega_1)t-\frac{\omega_o+\omega_1}{2}\cos(\omega_o+\omega_1)t\right)dt}{\int_0^T (\sin^2\omega_o t+\sin^2\omega_1 t+\sin(\omega_o-\omega_1)t-\sin(\omega_o+\omega_1)t)dt} \tag{4.113}$$

Comparison of (4.112) and (4.113) shows that the behavior of the proposed device is very similar to that of Ciciora's for an input consisting of two cosine waves. The terms at the sum and difference frequencies arise from mixing in the non-linear elements of the estimators. In Ciciora's device (equation (4.112)), the amplitude of these mixing terms in the numerator integral is $\sqrt{\omega_o\omega_1}$, the geometric mean of ω_o and ω_1. In the proposed device (equation (4.113)), it is $(\omega_o+\omega_1)/2$, their arithmetic mean. If $\omega_o \neq \omega_1$, this is larger than the geometric mean, but the difference becomes smaller as the bandwidth of the input signal decreases.

Denenberg's estimator is again perfect, even for the case of a two-cosine-wave input. In equation (4.110), the

numerator and denominator integrands can both be factored, leaving

$$2\pi\hat{f} = \frac{\omega_o+\omega_1}{2}\,\frac{\int_0^T (1+\cos(\omega_o-\omega_1)t)\,dt}{\int_0^T (1+\cos(\omega_o-\omega_1)t)\,dt} = \frac{\omega_o+\omega_1}{2}\,. \tag{4.114}$$

This is not true for the case of three or more input frequencies, and, therefore, the equation should be in the form of (4.110) when being compared with (4.112) and (4.113). It is seen that the terms corresponding to the sum frequency $\omega_o+\omega_1$ are missing from both the numerator and denominator of (4.110). Also, the terms giving rise to the desired ratio $(\omega_o+\omega_1)/2$ are constants in (4.110); they are multiplied by either a $\sin^2$ term or a $\cos^2$ term in (4.112) and (4.113). This comparison is similar for any ϕ_{ok} and ϕ_{1k} in the input

$$v_A^k(t) = \cos(\omega_o t+\phi_{ok}) + \cos(\omega_1 t+\phi_{1k})\,. \tag{4.115}$$

Hence Denenberg's estimator, with its relative complexity (see Fig. 5), can be expected to be better than the other two. In order to answer the question of how much better, consider the case of an input spectrum which is flat between 300 Hz and 400 Hz and zero elsewhere (Fig. 9). This is a typical bandwidth for signals received by meteorological radars in a rainstorm.

From (4.12) and (4.13), in Ciciora's device

$$S_{CC}(\omega) = 2\pi(\tilde{R}_{AA}^2(0))\delta(\omega) + 2\left(|\omega|S_{AA}(\omega)\right) * \left(|\omega|S_{AA}(\omega)\right)$$

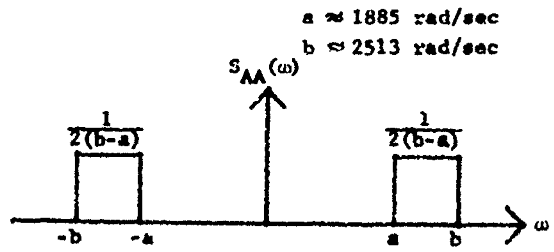

Fig. 9. Sample Input Spectrum

$$S_{EE}(\omega) = 2\pi(\check{R}_{AA}^2(0))\delta(\omega) + 2S_{AA}(\omega) * S_{AA}(\omega) \tag{4.116}$$

From (3.37) and (4.55), the average frequency of the input is given by

$$\bar{f} = \frac{\check{R}_{AA}^2(0)}{2\pi R_{AA}^2(0)} \tag{4.117}$$

Hence, in equation (4.116) the D.C. terms (those containing $\delta(\omega)$) are "signal" terms while the remaining terms give rise to noise, or error, in the estimate. For comparison, the spectra at similar points in he other estimators are given below. In Denenberg's device, from (4.62) and (4.67),

$$\begin{aligned} S_{MM}(\omega) = {} & 8\pi\check{R}_{AA}^2(0)\delta(\omega) + 2S_{AA}(\omega) * \omega^2 S_{AA}(\omega) \\ & + 2\left(|\omega|S_{AA}(\omega)\right) * \left(|\omega|S_{AA}(\omega)\right) \\ & + 2(\omega S_{AA}(\omega)) * (\omega S_{AA}(\omega)) \\ & - 2(\omega^2 W(\omega)S_{AA}(\omega)) * (W(\omega)S_{AA}(\omega)) \end{aligned} \tag{4.118}$$

$S_{QQ}(\omega) =$

$$8\pi R_{AA}^2(0)\delta(\omega) + 4S_{AA}(\omega) * S_{AA}(\omega) - 4(W(\omega)S_{AA}(\omega)) * (W(\omega)S_{AA}(\omega))$$

where $W(\omega)$ is given by (4.60).

In the proposed device, from (4.33), (4.68), and (4.13),

$S_{KK}(\omega) =$

$$2\pi \mathring{R}_{AA}^2(0)\delta(\omega) + S_{AA}(\omega) * \omega^2 S_{AA}(\omega) + \left(|\omega| S_{AA}(\omega)\right) * \left(|\omega| S_{AA}(\omega)\right)$$

$$S_{PP}(\omega) = 2\pi R_{AA}(0)\delta(\omega) + 2S_{AA}(\omega) * S_{AA}(\omega) \qquad (4.119)$$

All of these signals are processed by low-pass filters. It is assumed that these filters are the same for all three devices. Therefore, the signals are here compared at the filter inputs.

For the example shown in Fig. 8, it suffices to compare the noise spectra in the range $0 < \omega < (b-a)$, since in this example $(b-a)$ is 100 Hz, and the bandwidth of the low-pass filters is considerably smaller than that. Also, in equations (4.118) for Denenberg's device, it is seen that the D.C. terms in both the numerator ($S_{MM}(\omega)$) and denominator ($S_{QQ}(\omega)$) are four times those of the corresponding equations (4.116) and (4.119). Therefore, equations (4.118) should be divided by four for comparison with the others. In the range $0 < \omega < (b-a)$, by simple convolution,

$$\left(|\omega| S_{AA}(\omega)\right) * \left(|\omega| S_{AA}(\omega)\right) = -\omega S_{AA}(\omega) * \omega S_{AA}(\omega) =$$

$$\frac{1}{6(b-a)^2}\left((b^3 - a^3 - \omega^3) - 3a\omega(a+\omega)\right)$$

$$S_{AA}(\omega) * S_{AA}(\omega) = -W(\omega)S_{AA}(\omega) * W(\omega)S_{AA}(\omega) =$$

$$\frac{1}{2(b-a)^2}(b-a-\omega) \qquad (4.120)$$

$$S_{AA}(\omega) * \omega^2 S_{AA}(\omega) = -W(\omega)S_{AA}(\omega) * \omega^2 W(\omega)S_{AA}(\omega) =$$

$$\frac{1}{12(b-a)^2}\left(2(b^3-a^3) - 3\omega(a^2+b^2) + 3\omega^2(b-a) - 2\omega^3\right) .$$

Substituting this in (4.15), (4.17), and (4.18) gives, for Ciciora's device in the range $0 < \omega < (b-a)$,

$$S_{CC}(\omega) = \frac{1}{3(b-a)^2}\left((b^3-a^3-\omega^3) - 3a\omega(a+\omega)\right)$$

$$S_{EE}(\omega) = \frac{1}{(b-a)^2}(b-a-\omega) \qquad (4.121)$$

For Denenberg's device in this range,

$$\frac{1}{4}S_{MM}(\omega) = \frac{1}{3(b-a)^2}\left(2(b^3-a^3) - 3\omega(a^2+\omega^2) + 3\omega^2(b-a) - 2\omega^3\right)$$

$$\frac{1}{4}S_{QQ}(\omega) = \frac{1}{(b-a)^2}(b-a-\omega) , \qquad (4.122)$$

and for the proposed device in the same range,

$$S_{KK}(\omega) = \frac{1}{12(b-a)^2}\left(4(b^3-a^3-\omega^3) - 9(a^2\omega+a\omega^2) + 3(\omega^2 b-\omega b^2)\right)$$

$$S_{PP}(\omega) \quad \frac{1}{(b-a)^2}(b-a-\omega) \qquad (4.123)$$

The spectra of the numerator signals before filtering are plotted in Fig. 10. It is seen that the spectrum for the

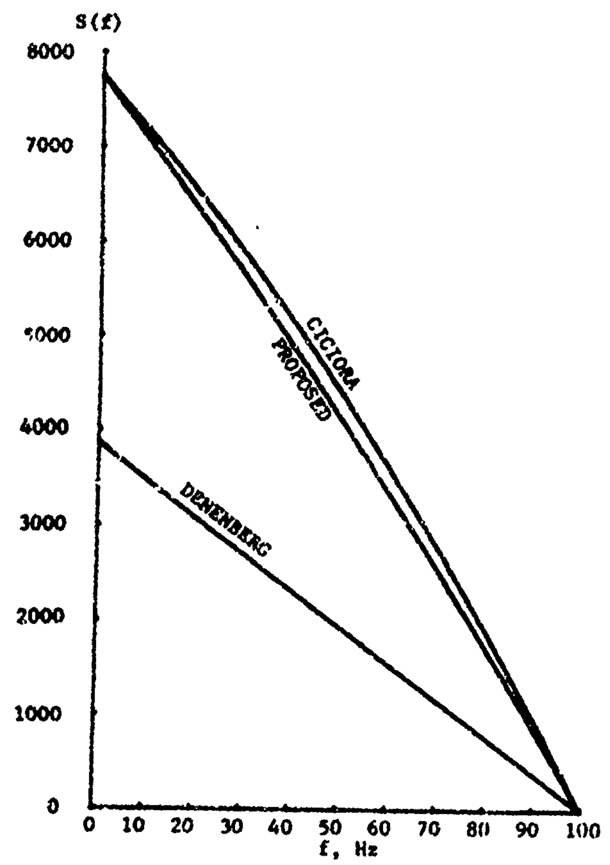

Fig. 10. Spectrum of Numerator Before Filtering

proposed device is very similar to that of Ciciora's, while Denenberg's device has only one-half as much noise in the numerator. This is true because, in equation (4.118), the terms $2\left(\left|\omega\right|S_{AA}(\omega)\right) * \left(\left|\omega\right|S_{AA}(\omega)\right)$ and $2(\omega S_{AA}(\omega)) * (\omega S_{AA}(\omega))$ add to zero in the range $0 < \omega < (b-a)$. As can be seen from equations (4.121) through (4.123) and from Fig. 11, the denominator spectra are the same for all three estimators.

The signal-to-noise ratio at the numerator can be calculated by recalling that the average (D.C.) value of the denominator signal in all three devices is an estimate of the input power. For the example of Fig. 9, this power is unity. Hence, the average value of the numerator is an estimate of the average radian frequency, which in this example is $2\pi(350)$ or 700π; the <u>power</u> at D.C. is, therefore, $(700\pi)^2$. This is the "signal" power; the noise power in the numerator depends on the bandwidth of the filter. For bandwidths up to 10 Hz, the power spectral density curves in Fig. 10 can be replaced by straight lines between the end points. The value at $f = 0$ for Ciciora's device and the proposed device is 7749.3. Recall that the noise spectrum is two-sided, and only one side is shown in Fig. 10. Then, if B is the bandwidth of the filter, the noise power after filtering is $15499B - 12.333B^2$. The noise for Denenberg's device is 3 db less. The signal-to-noise ratio of the numerator signals of the three devices at various filter bandwidths is shown in Table 1.

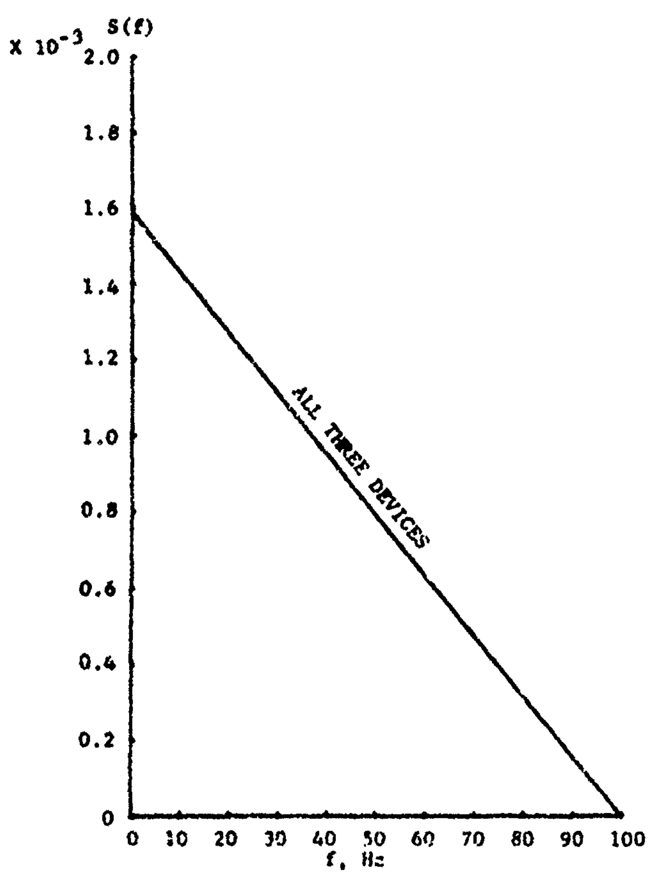

Fig. 11. Spectrum of Denominator Before Filtering

Table 1. Numerator S/N Ratio Versus Filter Bandwidth

Filter Bandwidth	Corresponding Integration Time T	S/N Ratio at D (Ciciora) and at U (Proposed)	S/N Ratio at S (Denenberg)
0.1 Hz	10.0 sec.	29.8 db	32.8 db
1.0	1.0	19.8	22.8
10.0	0.1	10.0	13.0

Unfortunately, knowledge of the signal-to-noise ratio of the numerator does not yield information about the quotient. However, the photographs in Chapter VI and the data in Appendix B show that the S/N ratio of the quotient is considerably better than that of the numerator.

Since nothing has been said of the power spectral density or the autocorrelation function at the divider outputs, analysis of a divider is considered in the next chapter.

CHAPTER V

PROBABILISTIC ANALYSIS WITH DIVIDER

This chapter discusses the possibility of extending the analysis of Chapter IV to the output divider, in order to obtain an expression for the autocorrelation function of the signal at the output. It is assumed that the autocorrelation functions for the divider inputs are known.

Let L, M, and Q denote the divider's numerator input, denominator input, and output, respectively. Define

$$\begin{aligned} v_1 &= v_L(t) \\ v_2 &= v_L(t+\tau) \\ v_3 &= v_M(t) \\ v_4 &= v_M(t+\tau) \ . \end{aligned} \tag{5.1}$$

It is first necessary to write an expression for $p_i(v_1,v_2,v_3,v_4)$, the joint probability density function of these four voltages. Assume for the moment that this function is joint gaussian with zero mean. (This point will be discussed later.) Then

$$p_i(v_1,v_2,v_3,v_4) = \frac{1}{4\pi^2|\Lambda|^{1/2}} \cdot \exp\left(\frac{-1}{2|\Lambda|}\sum_{i=1}^{4}\sum_{j=1}^{4}|\Lambda|_{ij}v_iv_j\right) , \tag{5.2}$$

where Λ is the covariance matrix of the input voltages, and $|\Lambda|_{ij}$ is the (i,j)-th cofactor, or signed minor, of Λ.

Define new random variables y_1 through y_4 as follows:

$$\begin{aligned} y_1 &= v_Q(t) = v_1/v_3 \\ y_2 &= v_Q(t+\tau) = v_2/v_4 \\ y_3 &= v_3 \\ y_4 &= v_4 \ . \end{aligned} \tag{5.3}$$

Solving (5.3) for v_1 through v_4 gives

$$\begin{aligned} v_1 &= y_1y_3 \\ v_2 &= y_2y_4 \\ v_3 &= y_3 \\ v_4 &= y_4 \ . \end{aligned} \tag{5.4}$$

By the standard fourth-order transformation of random variables, the joint probability density function for y_1 through y_4 is given by

$$p_o(y_1,y_2,y_3,y_4) = p_i(y_1y_3,y_2y_4,y_3,y_4)\,|J| \tag{5.5}$$

where

$$J = \begin{vmatrix} \frac{\partial v_1}{\partial y_1} & \frac{\partial v_2}{\partial y_1} & \frac{\partial v_3}{\partial y_1} & \frac{\partial v_4}{\partial y_1} \\ \frac{\partial v_1}{\partial y_2} & \frac{\partial v_2}{\partial y_2} & \frac{\partial v_3}{\partial y_2} & \frac{\partial v_4}{\partial y_2} \\ \frac{\partial v_1}{\partial y_3} & \frac{\partial v_2}{\partial y_3} & \frac{\partial v_3}{\partial y_3} & \frac{\partial v_4}{\partial y_3} \\ \frac{\partial v_1}{\partial y_4} & \frac{\partial v_2}{\partial y_4} & \frac{\partial v_3}{\partial y_4} & \frac{\partial v_4}{\partial y_4} \end{vmatrix} = \begin{vmatrix} y_3 & 0 & 0 & 0 \\ 0 & y_4 & 0 & 0 \\ y_1 & 0 & 1 & 0 \\ 0 & y_2 & 0 & 1 \end{vmatrix} = y_3y_4 \tag{5.6}$$

and thus

$$|J| \cdot |y_3 y_4| \quad . \tag{5.7}$$

Since p_1 is known, p_o is also known. F[illegible] the autocorrelation function of the output, however, it is necessary to find the second-order probability density function $p_Q(y_1,y_2)$. This is given by

$$p_Q(y_1,y_2) = \int_{-\infty}^{\infty}\int_{-\infty}^{\infty} p_o(y_1,y_2,y_3,y_4)\,dy_3 dy_4 \ , \tag{5.8}$$

where it is at least theoretically possible to carry out the integration.

Since $p_Q(y_1,y_2)$ is, by definition of y_1 and y_2, $p_Q(v_Q(t),v_Q(t+\tau))$, the autocorrelation function at Q is given by

$$R_{QQ}(\tau) = E[y_1 y_2] = \int_{-\infty}^{\infty}\int_{-\infty}^{\infty} y_1 y_2 p_Q(y_1,y_2)\,dy_1 dy_2 \ . \tag{5.9}$$

Hence, the autocorrelation function at the divider output is known, at least in terms of integrals. When the integrals are too difficult to carry out analytically, they can be evaluated by numerical methods on a digital computer.

In the proposed device, the bandwidth of the low-pass filters at the divider inputs is about 1 Hz, while a typical value for the bandwidth of the filter inputs is 50 Hz. Therefore, the integrators or low-pass filters sum approximately fifty statistically-independent values of their input voltages. Hence, an extension of the Central Limit Theorem can be used to establish that the signals at the filter outputs (divider inputs) are nearly gaussian, as assumed in (5.2).

A difficulty arises, however, in attempting to apply (5.2) to the proposed device. While the autocorrelation function at each divider input is known, the cross-correlation between the two inputs is unknown, and, hence, the covariance matrix Λ contains unknown members.

A device similar to the proposed device, designed to circumvent this difficulty, is now considered. Although no claim is made that this device is equivalent to the proposed one, it is here introduced to show how the above analysis might be applied to a complete system.

Figure 12 shows the proposed device. In Chapter VI, Fig. 24 shows that, even before integrating, the signal in the upper channel (numerator) is nearly a constant times the signal in the lower channel (denominator). Hence, it is feasible to divide these two signals first and then integrate over time. If this is done, the device becomes as shown in Fig. 13 and readily simplifies to the device of Fig. 14.

In this case, the cross-correlation between the divider inputs is already known. Equations (4.27) and (4.29) are directly applicable, and

$$R_{JH}(\tau) = R_{HJ}(\tau) = \overset{\vee}{R}_{AA}(\tau) \ . \tag{5.10}$$

Hence, the covariance matrix Λ in (5.2) is known, and thus the entire device is analyzed in terms of the input autocorrelation function. It may, however, be necessary to use a computer to carry out the integrations indicated in (5.8) and (5.9).

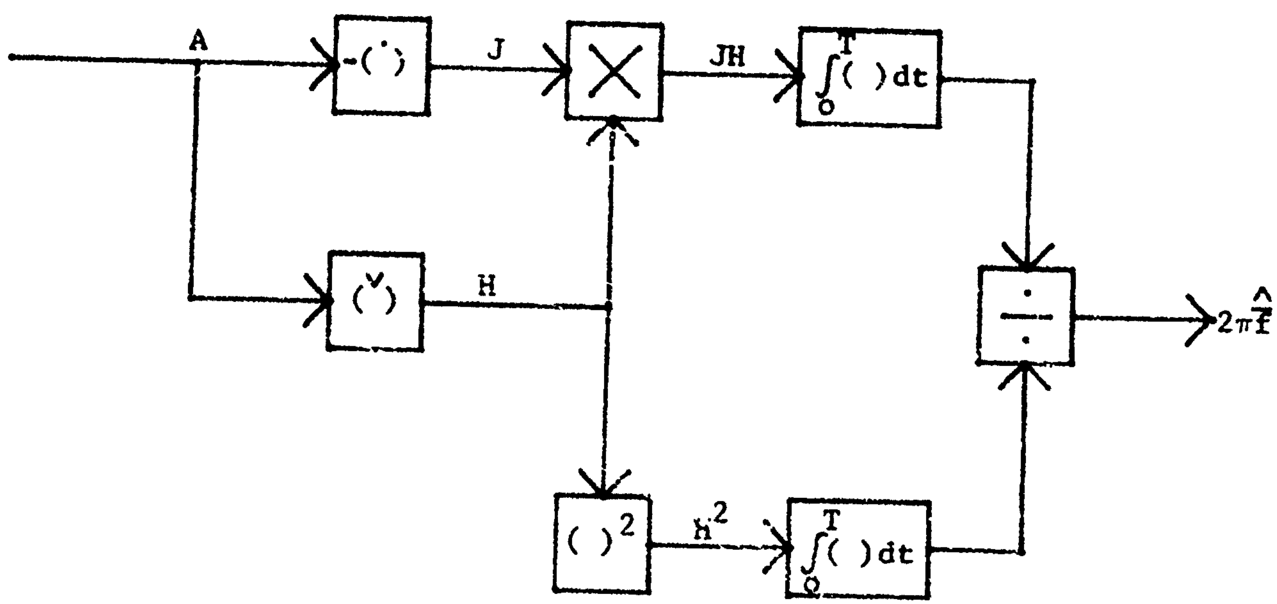

Fig. 12. Proposed Device

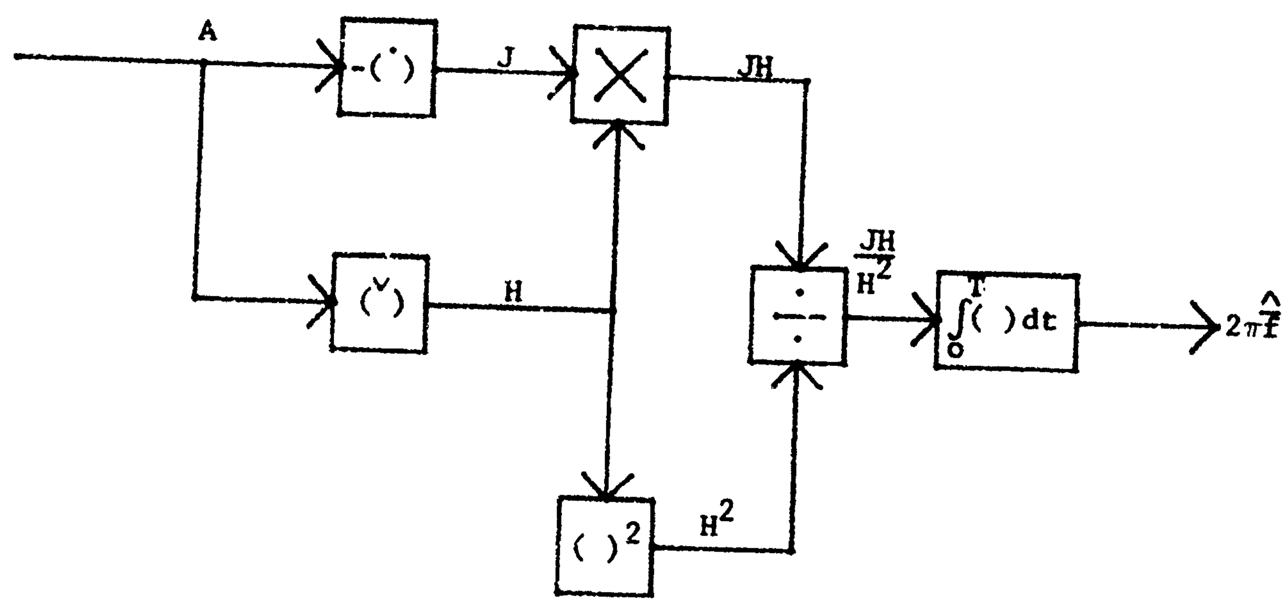

Fig. 13. Device Similar to That Proposed

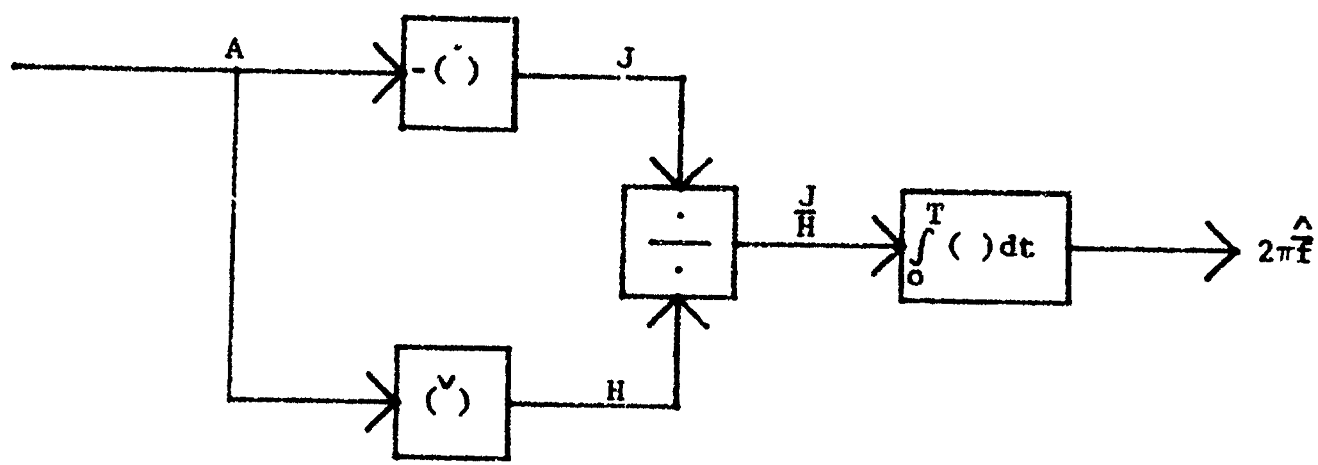

Fig. 14. Device of Fig. 13, Simplified

If the integrating time T is large, approximate expressions can be obtained for the bias and variance of the proposed estimate by making use of the power series approximation to $1/1+x$, where $|x| << 1$. Let $r_{XA}(\tau) = \hat{R}_{XA}(\tau) - R_{XA}(\tau)$ be the error in the estimate $\hat{R}_{XA}(\tau)$. Similarly, let $r_{XX}(\tau)$ be the error in $\hat{R}_{XX}(\tau)$. From (3.38), the proposed estimator is given by

$$-2\pi\hat{T} = \frac{\hat{R}_{XA}(0)}{\hat{R}_{XX}(0)} = \frac{R_{XA}(0) + r_{XA}(0)}{R_{XX}(0) + r_{XX}(0)} \quad (5.11)$$

If $|r_{XX}(0)| < |R_{XX}(0)|$, then

$$-2\pi\hat{T} = \frac{R_{XA}(0) + r_{XA}(0)}{R_{XX}(0)} \sum_{k=0}^{\infty} \left(-\frac{r_{XX}(0)}{R_{XX}(0)}\right)^k . \quad (5.12)$$

This is the power series expansion for $1/1+(r_{XX}(0)/R_{XX}(0))$. Expanding (5.12) and regrouping gives

$$-2\pi\hat{T} = \frac{R_{XA}(0)}{R_{XX}(0)} + \sum_{k=1}^{\infty}\left(-\frac{1}{R_{XX}(0)}\right)^k \left[\frac{R_{XA}(0)}{R_{XX}(0)}(r_{XX}(0))^k - r_{XA}(0)(r_{XX}(0))^{k-1}\right] . \quad (5.13)$$

If the integrating time is large, $|r_{XX}(0)/R_{XX}(0)| << 1$, and the above series can be approximated by its first two terms. Also, if P is the power in the input signal, then $R_{XX}(0) = P$ and $R_{XA}(0) = 2\pi TP$. Equation (5.13) then gives

$$\hat{T} - T \simeq -\frac{1}{P}\left[T r_{XX}(0) - \frac{r_{XA}(0)}{-2\pi}\right] + \frac{1}{P^2}\left[T r_{XX}^2(0) - \frac{r_{XA}(0) r_{XX}(0)}{-2\pi}\right] . \quad (5.14)$$

Retaining only the first term in (5.14) and squaring gives

$$(\hat{T}-T)^2 \simeq \frac{1}{P^2}\left[T^2 r_{XX}^2(0) - 2T r_{XX}(0)\left(\frac{r_{XA}(0)}{-2\pi}\right) + \left(\frac{r_{XA}(0)}{-2\pi}\right)^2\right] . \quad (5.15)$$

In order to calculate the bias and variance of the estimate of T, it is necessary to take the expected value of each term in (5.14) and (5.15). To find the expected value of $r_{XX}(0)$, write

$$\hat{R}_{XX}(\tau) = \frac{1}{T}\int_0^T \check{v}_A(t)\check{v}_A(t+\tau)\,dt . \quad (5.16)$$

Note that the right-hand side is an estimate of the time autocorrelation function $\mathcal{R}_{XX}(\tau)$. However, under the ergodic assumption, $\mathcal{R}_{XX}(\tau) = R_{XX}(\tau)$, and thus the right-hand side of (5.16) is also an estimate of the ensemble autocorrelation function $R_{XX}(\tau)$. Taking the expected value of both sides and interchanging the order of averaging and integration gives

$$E\left[\hat{R}_{XX}(\tau)\right] = \frac{1}{T}\int_0^T E\left[\check{v}_A(t)\check{v}_A(t+\tau)\right] dt \quad (5.17)$$

or

$$E\left[\hat{R}_{XX}(\tau)\right] = \frac{1}{T}\int_0^T R_{XX}(\tau)\,dt = R_{XX}(\tau) . \quad (5.18)$$

Therefore,

$$E\left[r_{XX}(\tau)\right] = 0 . \quad (5.19)$$

Similarly,

$$E\left[r_{X\dot{A}}(\tau)\right] = 0 \; . \tag{5.20}$$

This result states that the time-limited estimator of the autocorrelation function (equation (5.16)) is unbiased. This is a reasonable result, because for an ergodic (and, therefore, stationary) process, integrating for a limited time and averaging over an entire ensemble is equivalent to integrating a single sample function over all time.

To find the expected value of $r^2_{XX}(0)$, write

$$\hat{R}_{XX}(0) = \frac{1}{T}\int_{-T/2}^{T/2} V^2_A(t)\,dt \; . \tag{5.21}$$

Since the process is stationary, the integral shown above is equivalent to an integral from zero to T, as shown earlier. Squaring (5.21) gives

$$\hat{R}^2_{XX}(0) = \frac{1}{T^2}\int_{-T/2}^{T/2} V^2_A(t)\,dt \int_{-T/2}^{T/2} V^2_A(\tau)\,d\tau \tag{5.22}$$

or

$$\hat{R}^2_{XX}(0) = \frac{1}{T^2}\int_{-T/2}^{T/2}\int_{-T/2}^{T/2} V_A(t)V_A(t)V_A(\tau)V_A(\tau)\,d\tau\,dt \; , \tag{5.23}$$

Taking the expected value of both sides and making use of (4.26) gives

$$E\left[\hat{R}^2_{XX}(0)\right] = \frac{1}{T^2}\int_{-T/2}^{T/2}\int_{-T/2}^{T/2} R^2_{XX}(0) + 2R^2_{XX}(\tau-t)\,d\tau\,dt \; . \tag{5.24}$$

Taking the constant $R^2_{XX}(0)$ outside the integral gives

$$E\left[\hat{R}^2_{XX}(0)\right] - R^2_{XX}(0) = \frac{1}{T^2}\int_{-T/2}^{T/2}\int_{-T/2}^{T/2} 2R^2_{XX}(\tau-t)\,d\tau\,dt \; . \tag{5.25}$$

Recognizing the left-hand side as $E\left[r^2_{XX}(0)\right]$ and substituting $U = T/2$ in the right-hand side gives

$$E\left[r^2_{XX}(0)\right] = \frac{1}{4U^2}\int_{-U}^{U}\int_{-U}^{U} 2R^2_{XX}(\tau-t)\,d\tau\,dt \; . \tag{5.26}$$

Note that the substitution made above is <u>not</u> a change in the variables of integration, but only a substitution $U = T/2$ in the limits. Since the integrand is an even function of τ-t, a development by Davenport and Root[4] applies, and (5.26) leads to

$$E\left[r^2_{XX}(0)\right] = \frac{2}{U}\int_{0}^{2U}\left(1 - \frac{\tau}{2U}\right)R^2_{XX}(\tau)\,d\tau \tag{5.27}$$

or, since $U = T/2$ and $R_{XX}(\tau) = R_{AA}(\tau)$,

$$E\left[r^2_{XX}(0)\right] = \frac{4}{T}\int_{0}^{T}\left(1 - \frac{\tau}{T}\right)R^2_{AA}(\tau)\,d\tau \; . \tag{5.28}$$

To find $E\left[r_{XX}(0)\left\{r_{X\dot{A}}(0)/-2\pi\right\}\right]$ write

$$E\left[\hat{R}_{XX}(0)\frac{\hat{R}_{X\dot{A}}(0)}{-2\pi}\right] = R_{XX}(0)\,\frac{R_{X\dot{A}}(0)}{-2\pi} + \frac{R_{X\dot{A}}(0)}{-2\pi}\,E\left[r_{XX}(0)\right]$$
$$+ R_{XX}(0)\,E\left[\frac{r_{X\dot{A}}(0)}{-2\pi}\right] + E\left[r_{XX}(0)\,\frac{r_{X\dot{A}}(0)}{-2\pi}\right] \; . \tag{5.29}$$

Since $E\left[r_{XX}(0)\right] = E\left[r_{X\dot{A}}(0)\right] = 0$,

$$E\left[\hat{R}_{XX}(0)\frac{\hat{R}_{X\dot{A}}(0)}{-2\pi}\right] - R_{XX}(0)\frac{R_{X\dot{A}}(0)}{-2\pi} = E\left[r_{XX}(0)\frac{r_{X\dot{A}}(0)}{-2\pi}\right] \; . \tag{5.30}$$

$\hat{R}_{XX}(0)\left[\hat{R}_{X\dot{X}}(0)/-2\pi\right]$ can be written

$$\hat{R}_{XX}(0)\frac{\hat{R}_{X\dot{X}}(0)}{-2\pi} = \frac{1}{2\pi T^2}\int_{-T/2}^{T/2}\check{v}_A^2(t)\,dt\int_{-T/2}^{T/2}\check{v}_A(\tau)\dot{v}_A(\tau)\,d\tau$$

$$= -\frac{1}{2\pi T^2}\int_{-T/2}^{T/2}\check{v}_A(t)\check{v}_A(t)\check{v}_A(\tau)\dot{v}_A(\tau)\,d\tau\,dt \ . \qquad (5.31)$$

Taking the expected value of both sides and applying (4.23) gives

$$E\left[\hat{R}_{XX}(0)\frac{\hat{R}_{X\dot{X}}(0)}{-2\pi}\right] = -\frac{1}{2\pi T^2}\int_{-T/2}^{T/2}\int_{-T/2}^{T/2}\big(R_{XX}(0)R_{X\dot{X}}(0)$$

$$+ 2R_{XX}(\tau-t)R_{X\dot{X}}(\tau-t)\big)\,d\tau\,dt. \qquad (5.32)$$

Subtracting $R_{XX}(0)\left[R_{X\dot{X}}(0)/-2\pi\right]$ from both sides using (5.30) gives

$$E\left[r_{XX}(0)\frac{r_{X\dot{X}}(0)}{-2\pi}\right] = -\frac{1}{\pi T^2}\int_{-T/2}^{T/2}\int_{-T/2}^{T/2}R_{XX}(\tau-t)R_{X\dot{X}}(\tau-t)\,d\tau\,dt \ . \qquad (5.33)$$

From (4.50), $R_{X\dot{X}}(\tau) = -\dot{R}_{AA}(\tau)$. Therefore, the integrand in (5.33) is an even function of $\tau-t$. Substituting $U = T/2$, applying the development of Davenport and Root[4], and substituting $T/2$ for U, $R_{AA}(\tau)$ for $R_{XX}(\tau)$, and $-\dot{R}_{AA}(\tau)$ for $R_{X\dot{X}}(\tau)$ (see (4.46)), results in

$$E\left[r_{XX}(0)\frac{r_{X\dot{X}}(0)}{-2\pi}\right] = -\frac{4}{T}\int_0^T\left(1-\frac{\tau}{T}\right)\left(R_{AA}(\tau)\frac{\dot{R}_{AA}(\tau)}{-2\pi}\right)d\tau \ . \qquad (5.34)$$

A derivation exactly parallel with that of (5.27) results in

$$E\left[\left(\frac{r_{X\dot{X}}(0)}{-2\pi}\right)^2\right] = \frac{1}{\pi^2 T}\int_0^T\left(1-\frac{\tau}{T}\right)\dot{R}_{AA}^2(\tau)\,d\tau \ . \qquad (5.35)$$

Taking the expected value of (5.14) using (5.19), (5.20), (5.28), and (5.34) gives

$$E\left[\hat{\bar{f}}-\bar{f}\right] \approx \frac{4}{P^2 T}\left[\bar{f}\int_0^T\left(1-\frac{\tau}{T}\right)R_{AA}^2(\tau)\,d\tau\right.$$

$$\left.+\int_0^T\left(1-\frac{\tau}{T}\right)R_{AA}(\tau)\frac{\dot{R}_{AA}(\tau)}{-2\pi}\,d\tau\right] \ . \qquad (5.36)$$

The bias of the proposed estimator is then given approximately be

$$E\left[\hat{\bar{f}}-\bar{f}\right] \approx \frac{4}{P^2 T}\left[\int_0^T\left(1-\frac{\tau}{T}\right)\left(\bar{f}R_{AA}^2(\tau)-\frac{1}{2\pi}R_{AA}(\tau)\dot{R}_{AA}(\tau)\right)d\tau\right] \ . \qquad (5.37)$$

Taking the expected value of (5.15) using (5.28), (5.34), and (5.35) gives

$$E\left[(\hat{\bar{f}}-\bar{f})^2\right] \approx \frac{4}{P^2 T}\int_0^T\bar{f}^2\left(1-\frac{\tau}{T}\right)R_{AA}^2(\tau)\,d\tau$$

$$+\frac{8}{P^2 T}\int_0^T\bar{f}\left(1-\frac{\tau}{T}\right)R_{AA}(\tau)\frac{\dot{R}_{AA}(\tau)}{-2\pi}\,d\tau$$

$$+\frac{4}{P^2 T}\int_0^T\left(1-\frac{\tau}{T}\right)\left(\frac{\dot{R}_{AA}(\tau)}{-2\pi}\right)^2 d\tau \ . \qquad (5.38)$$

The variance of the proposed estimator is then given approximately by

$$E\left[(\hat{T}-\bar{T})^2\right] \approx \frac{4}{P^2 T}\int_0^T \left(\left(\bar{T}^2 R_{AA}^2(\tau) - \frac{1}{\pi}\bar{T} R_{AA}(\tau)\dot{R}_{AA}(\tau) + \frac{1}{4\pi^2}\dot{R}_{AA}^2(\tau)\right)\left(1-\frac{\tau}{T}\right)\right)d\tau \;. \tag{5.39}$$

In order to compare these results with Denenberg's estimator, the bias and variance of his estimate are now derived in terms of $R_{AA}(\tau)$, in a manner parallel with the derivation just given for the proposed estimator.

In Chapter III, equation (3.30) was derived from (3.14). Denenberg's estimator can, therefore, be expressed as

$$j2\pi\hat{T} = \frac{\hat{\dot{R}}_{ZZ}(0)}{\hat{R}_{ZZ}(0)} \;. \tag{5.40}$$

If $r_{ZZ}(\tau) = \hat{R}_{ZZ}(\tau) - R_{ZZ}(\tau)$ and $\dot{r}_{ZZ}(\tau) = \hat{\dot{R}}_{ZZ}(\tau) - \dot{R}_{ZZ}(\tau)$, then

$$j2\pi\hat{T} = \frac{\dot{R}_{ZZ}(0) + \dot{r}_{ZZ}(0)}{R_{ZZ}(0) + r_{ZZ}(0)} \;. \tag{5.41}$$

If $\left|r_{ZZ}(0)\right| < \left|R_{ZZ}(0)\right|$, (5.41) can be expanded in a power series similar to (5.13).

$$j2\pi\hat{T} = \frac{\dot{R}_{ZZ}(0)}{R_{ZZ}(0)} + \sum_{k=1}^{\infty}\left(-\frac{1}{R_{ZZ}(0)}\right)^k \left[\frac{\dot{R}_{ZZ}(0)}{R_{ZZ}(0)}\left(r_{ZZ}(0)\right)^k - \dot{r}_{ZZ}(0)\left(r_{ZZ}(0)\right)^{k-1}\right] \tag{5.42}$$

Since $R_{ZZ}(0) = 2P$, $\dot{R}_{ZZ}(0) = j4\pi\bar{T}P$ from (3.14). If the integrating time is large, $\left|r_{ZZ}(0)/R_{ZZ}(0)\right| \ll 1$, and the above series can be approximated by its first two terms. Equation (5.42) then gives

$$\hat{T}-\bar{T} \approx -\frac{1}{2P}\left[\bar{T}\, r_{ZZ}(0) - \frac{\dot{r}_{ZZ}(0)}{j2\pi}\right] + \frac{1}{4P^2}\left[\bar{T}\, r_{ZZ}^2(0) - \frac{\dot{r}_{ZZ}(0)}{j2\pi}\, r_{ZZ}(0)\right] \;. \tag{5.43}$$

Retaining only the first term and squaring gives

$$(\hat{T}-\bar{T})^2 \approx \frac{1}{4P^2}\left[\bar{T}^2 r_{ZZ}^2(0) - 2\bar{T}\, r_{ZZ}(0)\,\frac{\dot{r}_{ZZ}(0)}{j2\pi} + \left(\frac{\dot{r}_{ZZ}(0)}{j2\pi}\right)^2\right]. \tag{5.44}$$

It is next necessary to find the expected value of each of the terms in (5.43) and (5.44). From (3.19) and the denominator of (3.29),

$$\hat{R}_{ZZ}(0) = \hat{R}_{AA}(0) + \hat{R}_{\check{X}\check{X}}(0) \;. \tag{5.45}$$

Therefore,

$$\begin{aligned}\hat{R}_{ZZ}^2(0) &= \left(\frac{1}{T}\int_{-T/2}^{T/2}(v_A^2(t) + \check{v}_A^2(t))\,dt\right)\left(\frac{1}{T}\int_{-T/2}^{T/2}(v_A^2(\tau) + \check{v}_A^2(\tau))\,d\tau\right)\\
&= \frac{1}{T^2}\int_{-T/2}^{T/2}\int_{-T/2}^{T/2}(v_A(t)v_A(t)v_A(\tau)v_A(\tau)\\
&\quad + v_A(t)v_A(t)\check{v}_A(\tau)\check{v}_A(\tau) + \check{v}_A(t)\check{v}_A(t)v_A(\tau)v_A(\tau)\\
&\quad + \check{v}_A(t)\check{v}_A(t)\check{v}_A(\tau)\check{v}_A(\tau))\,d\tau\, dt \;.\end{aligned} \tag{5.46}$$

The next step is to take the expected value of (5.46). After much straightforward algebra, applying (4.24) four times and making use of (4.19) and (4.28) results in

$$E\left[R_{ZZ}^2(0)\right] = \frac{4}{T^2}\int_{-T/2}^{T/2}\int_{-T/2}^{T/2}\left(R_{AA}^2(0) + R_{AA}^2(\tau-t) + \check{R}_{AA}^2(\tau-t)\right)d\tau dt \ . \qquad (5.47)$$

Subtracting $R_{ZZ}^2(0) = \left[2R_{AA}(0)\right]^2$ from (5.47) gives

$$E\left[r_{ZZ}^2(0)\right] = \frac{4}{T^2}\int_{-T/2}^{T/2}\int_{-T/2}^{T/2}\left(R_{AA}^2(\tau-t) + R_{AA}^2(\tau-t)\right)d\tau dt \ . \qquad (5.48)$$

Since the integrand is even, the substitution $U = T/2$ in the limits makes the development of Davenport and Root[4] applicable. The result is

$$E\left[r_{ZZ}^2(0)\right] = \frac{8}{T}\int_0^T\left|1 - \frac{\tau}{T}\right|\left(R_{AA}^2(\tau) + \check{R}_{AA}^2(\tau)\right)d\tau \ . \qquad (5.49)$$

Since $E\left[r_{ZZ}(0)\right] = E\left[\hat{r}_{ZZ}(0)\right] = 0$,

$$E\left[\hat{R}_{ZZ}(0)\frac{\dot{\hat{R}}_{ZZ}(0)}{j}\right] = R_{ZZ}(0)\frac{\dot{R}_{ZZ}(0)}{j} + E\left[r_{ZZ}(0)\frac{\dot{r}_{ZZ}(0)}{j}\right] \ . \qquad (5.50)$$

Consider equation (3.24) and the numerator of (3.29). $R_{ZZ}(0)(\dot{R}_{ZZ}(0)/j)$ can be written

$$\hat{R}_{ZZ}(0)\frac{\hat{R}_{ZZ}(0)}{j} = \left(\frac{1}{T}\int_{-T/2}^{T/2}\left(v_A^2(t) + \check{v}_A^2(t)\right)dt\right)$$

$$\left(\frac{1}{T}\int_{-T/2}^{T/2}\left(v_A(\tau)\dot{\check{v}}_A(\tau) - \check{v}_A(\tau)\dot{v}_A(\tau)\right)d\tau\right)$$

$$= \frac{1}{T^2}\int_{-T/2}^{T/2}\int_{-T/2}^{T/2}\left(v_A(t)v_A(t)v_A(\tau)\dot{\check{v}}_A(\tau) - v_A(t)v_A(t)\check{v}_A(\tau)\dot{v}_A(\tau)\right.$$

$$\left. + \check{v}_A(t)\check{v}_A(t)v_A(\tau)\dot{\check{v}}_A(\tau) - \check{v}_A(t)\check{v}_A(t)\check{v}_A(\tau)\dot{v}_A(\tau)\right)d\tau dt \qquad (5.51)$$

The expected value of this expression can be taken by applying (4.24) four times and making use of (4.19), (4.55), (4.50), (4.48), and (4.51). The result is

$$E\left[\hat{R}_{ZZ}(0)\frac{\dot{\hat{R}}_{ZZ}(0)}{j}\right] = \frac{4}{T^2}\int_{-T/2}^{T/2}\int_{-T/2}^{T/2}\left(R_{AA}(0)\dot{\check{R}}_{AA}(0)\right.$$

$$\left. + R_{AA}(\tau-t)\dot{\check{R}}_{AA}(\tau-t) - \check{R}_{AA}(\tau-t)\dot{R}_{AA}(\tau-t)\right)d\tau dt \ . \qquad (5.52)$$

From (3.24), (4.50), and (4.55), $(\dot{R}_{ZZ}(0)/j) = 2\dot{\check{R}}_{AA}(0)$. Also, from (3.33), $R_{ZZ}(0) = 2R_{AA}(0)$. Subtracting (5.50) from (5.52), therefore, gives

$$E\left[r_{ZZ}(0)\frac{\dot{r}_{ZZ}(0)}{j}\right] = \frac{4}{T^2}\int_{-T/2}^{T/2}\int_{-T/2}^{T/2}\left(R_{AA}(\tau-t)\dot{\check{R}}_{AA}(\tau-t)\right.$$

$$\left. - \check{R}_{AA}(\tau-t)\dot{R}_{AA}(\tau-t)\right)d\tau dt \ . \qquad (5.53)$$

Since the integrand is even, the substitution $U = T/2$ in the limits enables the development of Davenport and Root[4] to be applied. Therefore,

$$E\left[r_{ZZ}(0)\frac{\dot{r}_{ZZ}(0)}{j}\right] = \frac{8}{T}\int_0^T\left|1 - \frac{\tau}{T}\right|\left(R_{AA}(\tau)\dot{\check{R}}_{AA}(\tau) - \check{R}_{AA}(\tau)\dot{R}_{AA}(\tau)\right)d\tau \ . \qquad (5.54)$$

Finally, $(\dot{\hat{R}}_{ZZ}(0)/j)^2$ can be written

$$\left(\frac{\dot{\hat{R}}_{ZZ}(0)}{j}\right)^2 = \left(\frac{1}{T}\int_{-T/2}^{T/2}v_A(t)\dot{\check{v}}_A(t) - \check{v}_A(t)\dot{v}_A(t)dt\right)$$

$$\left(\frac{1}{T}\int_{-T/2}^{T/2}v_A(\tau)\dot{\check{v}}_A(\tau) - \check{v}_A(\tau)\dot{v}_A(\tau)d\tau\right)$$

$$- \frac{1}{T^2} \int_{-T/2}^{T/2} \int_{-T/2}^{T/2} \Big(v_A(t)\check{\check{v}}_A(t) v_A(\tau)\check{\check{v}}_A(\tau)$$

$$- v_A(t)\check{\check{v}}_A(t)\check{v}_A(\tau)\dot{v}_A(\tau) - \check{v}_A(t)\dot{v}_A(t)v_A(\tau)\check{\check{v}}_A(\tau)$$

$$+ \check{v}_A(t)\dot{v}_A(t)\check{v}_A(\tau)\dot{v}_A(\tau)\Big) d\tau dt \ . \qquad (5.55)$$

Taking the expected value and using (4.24), (4.55), (4.19), (4.47), (4.50), (4.48), (4.51), and (4.46) gives

$$E\left[\left(\frac{\hat{\check{R}}_{ZZ}(0)}{J}\right)^2\right] = \frac{2}{T^2} \int_{-T/2}^{T/2} \int_{-T/2}^{T/2} \Big(2\check{R}^2_{AA}(0) - R_{AA}(\tau-t)\ddot{R}_{AA}(\tau-t)$$

$$+ \check{R}^2_{AA}(\tau-t) - \check{R}_{AA}(\tau-t)\check{\check{R}}_{AA}(\tau-t) + \dot{R}^2_{AA}(\tau-t)\Big) d\tau dt \ . \qquad (5.56)$$

Subtracting $(R_{ZZ}(0)/J)^2 = (2R_{AA}(0))^2$ (see (3.24)) gives

$$E\left[\left(\frac{\dot{r}_{ZZ}(0)}{J}\right)^2\right] = \frac{2}{T^2} \int_{-T/2}^{T/2} \int_{-T/2}^{T/2} \Big(-R_{AA}(\tau-t)\ddot{R}_{AA}(\tau-t)$$

$$+ \check{\check{R}}^2_{AA}(\tau-t) - \check{R}_{AA}(\tau-t)\check{\check{R}}_{AA}(\tau-t) + \dot{R}^2_{AA}(\tau-t)\Big) d\tau dt \ . \qquad (5.57)$$

Since the integrand is even, the substitution $U = t/2$ and the development of Davenport and Root[4] gives

$$E\left[\left(\frac{\dot{r}_{ZZ}(0)}{J}\right)^2\right] = \frac{4}{T} \int_0^T \left(1 - \frac{\tau}{T}\right) \Big(-R_{AA}(\tau)\ddot{R}_{AA}(\tau) + \check{\check{R}}^2_{AA}(\tau)$$

$$- \check{R}_{AA}(\tau)\check{\check{R}}_{AA}(\tau) + \dot{R}^2_{AA}(\tau)\Big) d\tau \ . \qquad (5.58)$$

Using (5.49) and (5.54) to take the expected value of (5.43) gives, after simplification, the following approximate expression for the bias of Denenberg's estimate:

$$E\left[\hat{\bar{f}}-\bar{f}\right] \simeq \frac{2}{P^2 T} \left[\int_0^T \left(1 - \frac{\tau}{T}\right) \Big(\bar{f} R^2_{AA}(\tau) + \bar{f}\check{R}^2_{AA}(\tau)\right.$$

$$\left. - \frac{1}{2\pi}\Big(R_{AA}(\tau)\check{R}_{AA}(\tau) - \check{R}_{AA}(\tau)\dot{R}_{AA}(\tau)\Big)\Big) d\tau \right] \ . \qquad (5.59)$$

Similarly, (5.49), (5.54), and (5.58) can be used to take the expected value of (5.44). The result, after simplification, is the following approximate expression for the variance of Denenberg's estimator:

$$E\left[(\hat{\bar{f}}-\bar{f})^2\right] \simeq \frac{2}{P^2 T} \left[\int_0^T \left(1 - \frac{\tau}{T}\right) \Big(\bar{f}^2 R^2_{AA}(\tau) + \bar{f}^2 \check{R}^2_{AA}(\tau)\right.$$

$$- \frac{1}{\pi}\Big(\bar{f}\, R_{AA}(\tau)\check{R}_{AA}(\tau) - \bar{f}\, \check{R}_{AA}(\tau)\dot{R}_{AA}(\tau)\Big)$$

$$+ \frac{1}{8\pi^2}\Big(-R_{AA}(\tau)\ddot{R}_{AA}(\tau) + \check{R}^2_{AA}(\tau) - \check{R}_{AA}(\tau)\check{\check{R}}_{AA}(\tau)$$

$$\left. + \dot{R}^2_{AA}(\tau)\Big)\Big) d\tau \right] \ . \qquad (5.60)$$

Equations (5.59) and (5.60) are to be compared with the corresponding equations (5.37) and (5.39) for the proposed device. Since the relative performance of these estimators is not obvious from inspection of these equations, the proposed device was constructed in the laboratory and its performance was compared with analytical expressions for Denenberg's estimator.

CHAPTER VI

LABORATORY MODEL

In order to evaluate the performance of the proposed estimator, a laboratory model was constructed and tested under typical operating conditions. The purpose of this chapter is to enable the reader to duplicate the laboratory model, and to present the experimental results.

In the construction of the proposed device, two EIA model TR-20 analog computers were used. The analog computers performed all functions except generation of the narrow-band noise at the input, filtering of the quadrature detector outputs, and division of the integrator outputs. Wide-band gaussian noise was obtained from a General Radio noise source, and a G.R. Wave Analyzer was used as a narrow-band filter. The quadrature detector outputs were filtered by means of bridged-T RC filters to be discussed later. The integrator outputs were read on a digital voltmeter and later divided on a digital computer.

A block diagram of the laboratory model is shown in Fig. 15. Buffers are necessary at each multiplier input, because the multipliers present a non-linear load. Buffers are also necessary at the output of each T-notch filter, as the filters have high-impedance outputs.

Those who are familiar with the analog computer can duplicate the laboratory model directly from the block diagram of Fig. 11. Potentiometers may be inserted as convenient, in order to keep all signals levels below 10 volts

peak, to prevent saturation of the operational amplifiers. If a potentiometer is used at a multiplier input, it should be inserted ahead of the corresponding buffer.

The laboratory model can also be duplicated by referring to the illustration of a patch panel in Fig. 16. The rows have been labeled for reference, and the columns are already numbered on the panel.

Two such panels will be required. On panel number one, the following connections should be made: Q8-P1-D4-D8; P2-E4-E8; C4-M11; H4-V1-A11; V2-J4; L4-M12, A7-V6; B7-X7; G8-T13; H8-P10-V9; J8-V10; L8-T14; A13-P6; T12-P9; B11 through a 0.015 mfd capacitor to T11; B13 through a 0.27 mfd capacitor to M13, M13 through a 0.001 mfd capacitor to M14.

A 10-kHz T-notch filter is connected as follows: input to L4, output to Q3, ground to H3. Another identical filter is connected as follows: input to L3, output to W3, ground to H3. The input, output, and ground of a 20-kHz filter are connected to P4, Q5, and H3, respectively; another such filter is similarly connected to V4, W5, and H3. The audio oscillator is connected to V1, the narrow-band noise source to R7. The grounds on all equipment should be connected to H3. Three single jumper plugs are inserted at each of the three integrators, and double jumper plugs are inserted at operational amplifiers one through ten. Ten-kilohm resistors are inserted across operational amplifiers 12 and 13, but not across 11 and 14.

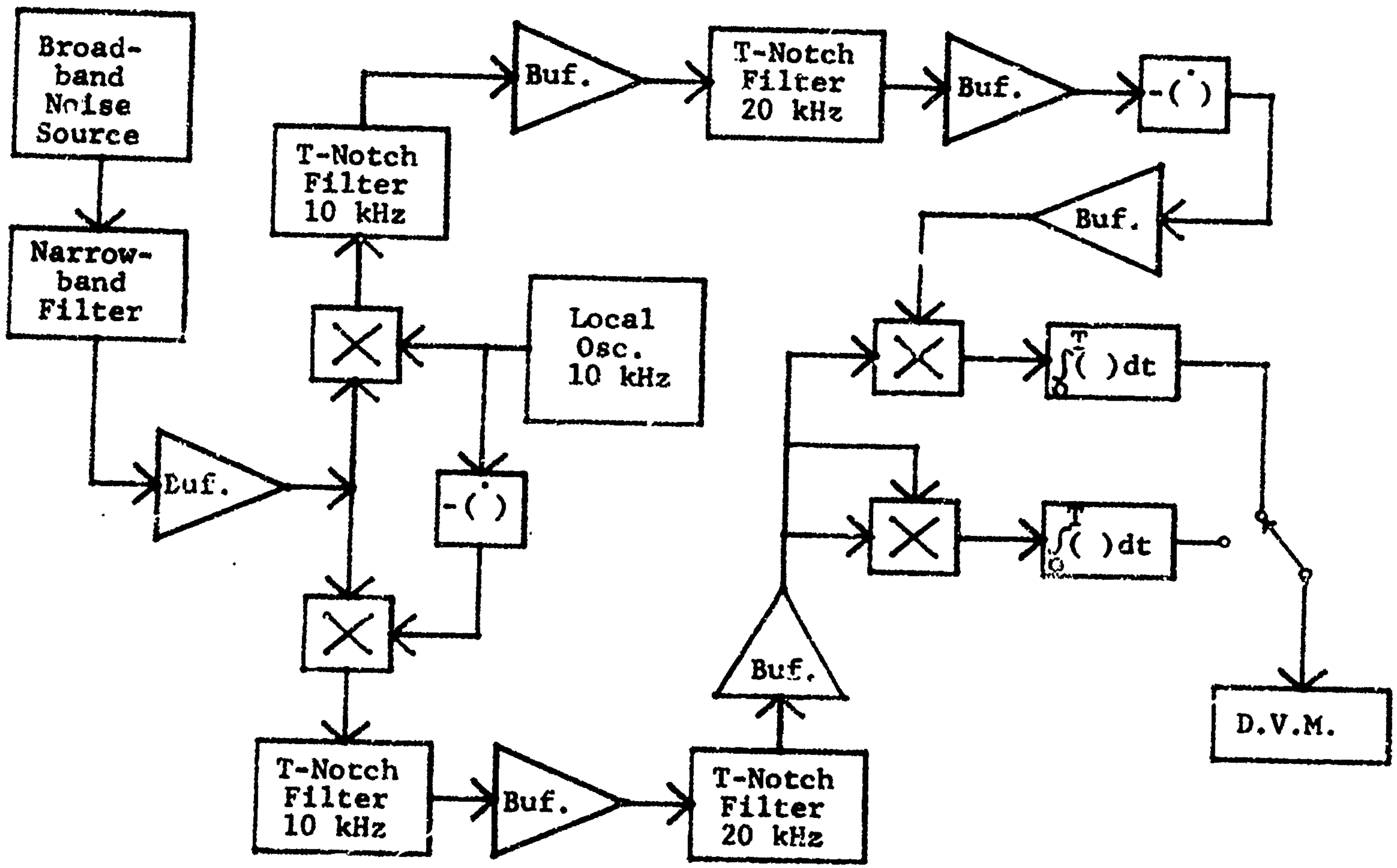

Fig. 15. Bl. .k Diagram of the Laboratory Model

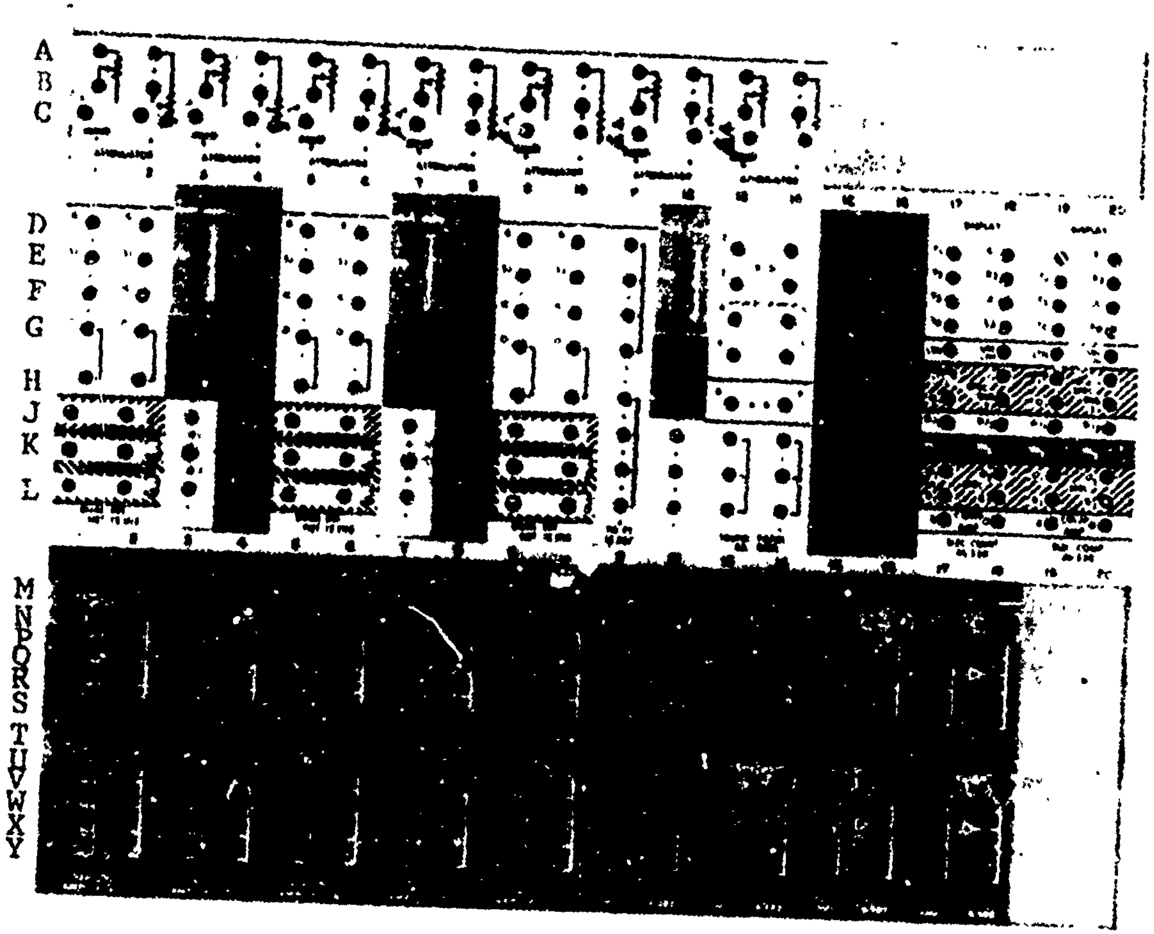

Fig. 16. Fatch Panel of EAI Model TR-20 Analog Computer

On panel number two, the following connections should be made: A7-Q6; B7-Q7, Q4-W7; D1-M4; E1-M3; F1-F1-G3, G1-N4: D2-M6; E2-M5; D4-V4, E4-P2; G2-N6, C4-M11; D8-H8-H4-W1; E3-J8-J4-W2; G8-T11; T12-L8-P5; M12-L4-P3; Q2-V3 The grounds on all equipment are connected to H3. Three single jumper plugs are inserted at each of the three integrators, and double jumper plugs are inserted at all operational amplifiers one through ten, except three and five. Ten-kilohm resistors are inserted across all remaining operational amplifiers except 11 and 12. The numerator and denominator outputs are obtained by switching a digital voltmeter between amplifiers eight and seven, respectively.

Connect G3 on panel one to G3 on panel two, M14 on one to R1 on two, and V8 on one to W1 on two.

The settings of the three potentiometers are recorded with the laboratory data in Appendix B.

The T-notch filters are designed to reject 10-kHz and 20-kHz energy from the quadrature detector. A schematic diagram is shown in Fig. 17. The following equations apply to the filters.

$$C_2 = 2C_1 = 2C_3 \qquad (6.1)$$

$$R_2 = R_3 = R_1/2 \qquad (6.2)$$

$$f = \frac{1}{2\pi R_1 C_1} , \qquad (6.3)$$

where f is the frequency to be rejected. Two 10-kHz filters and two 20-kHz filters are required R1 should be of the order of magnitude of 5,000 ohms. R2 and R3 are 1%-tolerance

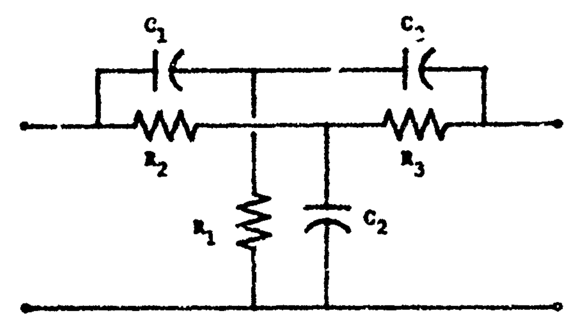

Fig. 17. T-Notch Filter (Four Required)

resistors, and a small potentiometer can be inserted in series with R1 to permit fine frequency adjustment. An accurate capacitance bridge should be used to select C1, C2, and C3 by hand to within a tolerance of one percent.

In operation, some overload lights on the analog computers are lit. Due to the relatively high frequencies involved, this does not necessarily mean that the operational amplifiers are being driven to saturation. The output of each operational amplifier should be observed with an oscilloscope, to make certain that no voltage exceeds 10 volts peak.

The two greatest difficulties encountered in the operation of the laboratory model were poor multiplier dynamic range and chopper noise. In order to overcome poor dynamic range, potentiometers were used to adjust the

multiplier input signals to values between 5 and 10 volts peak. A large change in the average frequency of the input necessitates readjustment of the signal levels.

Since the operational amplifiers are chopper-stabilized, noise is introduced into the system from this source. It is especially apparent at the output of the (negative) differentiator, a device which emphasizes high frequencies. Fortunately, the chopper noise is of very short duration and, therefore, causes only small errors at the integrator outputs.

Photographs of the waveforms at various points in the system are shown in Figs. 18 through 24. Fig. 18 shows the narrow-band input noise. Figure 19 shows the local oscillator signal and this signal shifted by 90 deg. This and all subsequent photographs were taken on a two-channel oscilloscope using the chopped mode. Figure 20 shows the two outputs of the quadrature detector before filtering. The 90-deg phase shift is apparent, and there is additive 10-kHz and 20-kHz energy. Figure 21 shows these same signals after filtering by the T-notch filters. Figure 22 shows the operation of the negative differentiator. The upper signal is its input and the lower signal its output. Figure 23 shows the output of the negative differentiator (top) and the second quadrature-detector output (bottom). This shows that, while the two quadrature-detector outputs differ in phase by 90 deg, they become in-phase when one is differentiated. Figure 24 shows the two integrator inputs. Note that one is

10 volts/div. 100 msec/div.

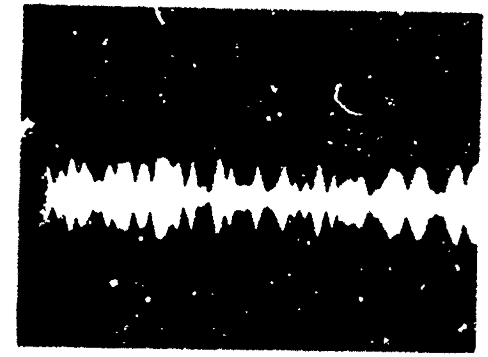

Fig. 18. Narrow-Band Input Noise

10 volts/div. 0.1 msec/div.

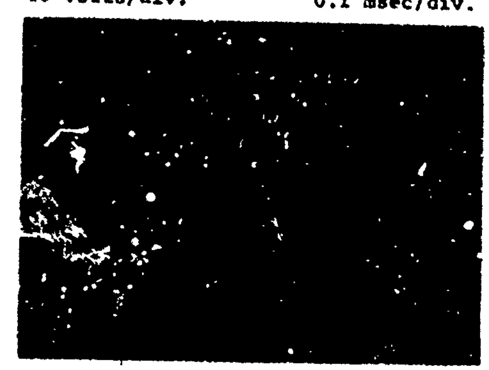

Fig. 19. · al Oscillator Signals

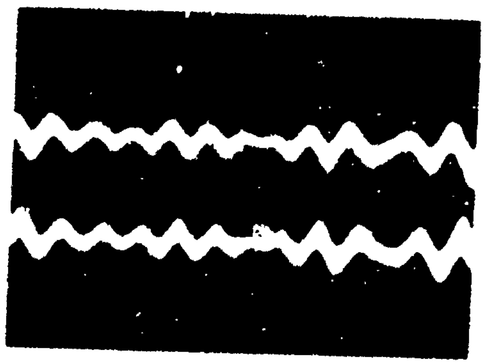

Fig. 20. Quadrature Detector Outputs Before Filtering

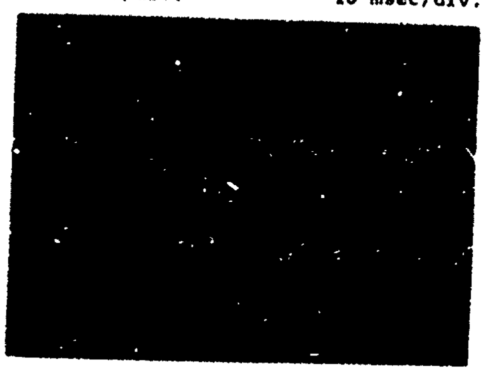

Fig. 21. Quadrature Detector Outputs After Filtering

Fig. 22. Input and Output of Negative Differentiator

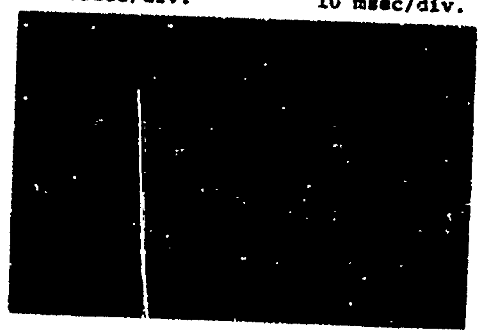

Fig. 23. Output of Negative Differentiator Versus Second Quadrature Detector Output

10 volts/div. 10 msec/div.

Fig. 24. Inputs to the Two Integrators

nearly a constant times the other. This explains why the process of division by a local estimate of the input power greatly reduces the variance of the estimate. It also provides some justification for introducing the alternate device in Chapter V, a device which divides before integration.

Figure 25 is a graph of the average quotient of the integrator outputs versus input average frequency. This graph demonstrates the linearity of the system. That is, the output is proportional to $\bar{f} - f_{LO}$, where f_{LO} is the frequency of the local oscillator. The + signs in Fig. 25 show the observed values of the output versus $\bar{f} - f_{LO}$. The coefficient of correlation between these two variables is 0.9993. The solid line shows the straight line of best fit

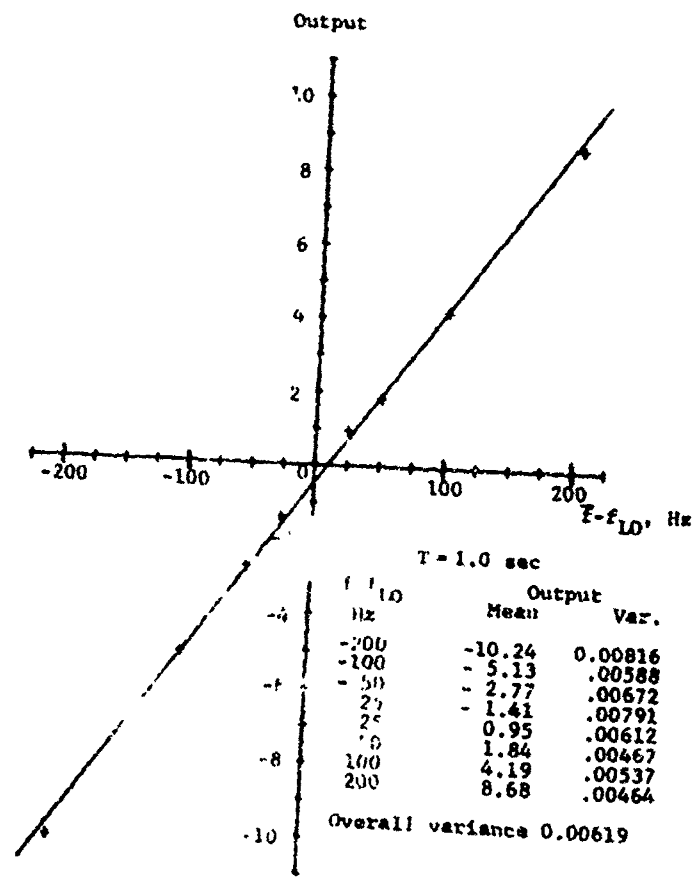

Fig. .5. ..inearity of the Estimator

using the least squares criterion This line has a slope of 0 04711 Hz^{-1} and a y-intercept of -0 48625.

For each set of operating conditions (input average frequency and averaging time), at least 50 determinations of the two integrator outputs were made These are recorded in Appendix B It is obvious that the quotient has a much smaller variance than the numerator. Thus, the process of division greatly improves the signal-to-noise ratio of the estimate For each of the first two runs, 100 determinations of the integrator outputs were made A digital computer was used to calculate the running mean and variance of the quotient after each ten measurements Examination of these results, which are given in Table 2, led to the conclusion that fifty runs provide a suitable basis for determining the mean and variance of the estimate. Fewer runs could have been used if only the mean were desired.

The overall variance for the eight sets of data at $T = 1.0$ sec is 0.00619. Since the slope of the graph in Fig 25 is 0 04711 Hz^{-1}, a variance of 0 00619 corresponds to 2 8 Hz^2 The variance at $T = 0$ 1 sec is 0 0714, which corresponds to 32 Hz^2. In all cases, the input consisted of wideband noise colored by a filter whose frequency response is given in Table 3

The laboratory results are easily compared with Denenberg's estimator The formula for the variance of his estimate is[7]

Table 2. Running Mean and Variance of the Estimate

$\bar{f} - f_{LO} = -100$ Hz, $T = 1.0$ sec			$\bar{f} - f_{LO} = -100$ Hz, $T = 0$ 1 sec		
Runs Used in Calculation	Calculated Mean	Calculated Variance	Runs Used in Calculation	Calculated Mean	Calculated Variance
First 10	-5.15	0.00480	First 10	-5.37	0.0536
First 20	-5.16	0.00403	First 20	-5.36	0.0573
First 30	-5.15	0.00431	First 30	-5 35	0.0675
First 40	-5.15	0.00541	First 40	-5.34	0.0700
First 50	-5.13	0.00655	First 50	-5.36	0.0678
First 60	-5.14	0.00693	First 60	-5.34	0.0642
First 70	-5.14	0.00625	First 70	-5.35	0.0661
First 80	-5.13	0.00641	First 80	-5.35	0 0684
First 90	-5.13	0.00614	First 90	-5.36	0.0672
All 100	-5.13	0.00[illegible]9	All 100	-5.38	0.0714

$$E\left[(\hat{\bar{f}}-\bar{f})^2\right] = \frac{\frac{1}{T}\int_0^{\infty} f^2 S_{AA}^2(f+\bar{f})\,df}{\int_0^{\infty} S_{AA}^2(f+\bar{f})\,df} \quad (6.4)$$

Carrying out the integrations by Simpson's Rule gives a variance of 2.66 Hz^2 for $T = 1.0$ sec and 26.6 Hz^2 at $T = 0.1$ sec. Thus, the variance of the proposed estimate is nearly the same as that of Denenberg's at ordinary averaging times (e.g., 1.0 sec); it becomes worse for small T (e.g., 0.1 sec).

Table 3. Frequency Response of Narrow-Band Filter

Displacement from Center Frequency, Hz	Relative Response, db	Displacement from Center Frequency, Hz	Relative Response, db
0	0.0	3	0.0
-7	-0.5	13	-0.5
-17	-1.3	23	-3.0
-27	-5.0	33	-7.8
-37	-10.0	43	-14.0
-47	-15.0	53	-20.0
-57	-21.0	63	-25.0
-67	-27.0	73	-30.0
-77	-31.0	83	-35.0
-87	-35.5	93	-39.0
-97	-39.0	103	-42.5
-107	-43.0	113	-45.5
-117	-46.5	123	-49.0
-127	-49.2	133	-52.0
-137	-52.5	143	-54.5
-147	-55.5	153	-57.0
-157	-57.5	163	-59.0
-167	-60.0	173	-61.2
-177	-62.5	183	-63.5
-187	-64.0	193	-65.0

CHAPTER VII

SUMMARY AND CONCLUSIONS

The field of radar meteorology provides a need for a device which measures the average frequency of a r[illegible] process. The literature search reveals that th[illegible]y ways to design such a device. Estimators proposed by Bello, Ciciora, and Denenberg are considered in detail. It is found that, for a simple rectangular window function, the estimators of Bello and Denenberg are identical.

Denenberg's estimator is re-derived using the Hilbert Transform (Appendix A). This derivation also leads to a new proposed estimator. It is found that, if a divider is appended to Ciciora's device, the signal spectra in the proposed device and in Ciciora's device are virtually identical. For a flat input spectrum, the low frequency noise in the numerator of Denenberg's estimator is about 3 db below that of the other two devices; the low frequency noise in the denominator is the same.

All three devices are analyzed, and expressions are obtained for the autocorrelation functions and power spectral densities at every point in each device up to the output divider. The divider is separately analyzed, and general expressions are obtained for these functions. The analysis is not directly applicable to the proposed estimator, however, because the cross-correlation function at the divider inputs is unknown. Another device which has a

known cross-correlation function is introduced, in order to show how the divider analysis might be applied.

By means of a power series approximation to division, approximate expressions are obtained for the bias and the variance of Denenberg's estimator and the proposed estimator.

A laboratory model of the proposed device is constructed, and measurements of the output are made for eight different input average frequencies, using an integrating time of one second. Additional measurements are made at one frequency, using a time of one-tenth second. It is found that the output is proportional to average frequency. The variance of the estimate is calculated. For an integrating time of one second, the variance is found to be about the same as that of Denenberg's estimator, but for a time of one-tenth second, the variance of the proposed estimator is noticeably greater than that of Denenberg's.

The following conclusions can be drawn:

Ciciora's estimator as originally proposed[2] will have a smaller variance if the output is divided by $\int_0^T v_A^2(t)dt$. In all three devices, the output divider will improve the signal-to-noise ratio.

Denenberg's estimator[5], which was obtained by frequency-domain considerations, is also derivable from time-domain considerations when the Hilbert transform is used. A new, simpler estimator is similarly derivable by these same considerations.

In all three devices, the power spectral density and autocorrelation function at any point except the output are expressible in terms of these same functions at the input. The power spectral density and autocorrelation function at the output are expressible in terms of integrals involving these same functions at the input, and the cross-correlation functions for the two divider inputs. Equations (5.59) and (5.60) give approximate expressions for the bias and the variance of Denenberg's estimator; equations (5.37) and (5.39) similarly pertain to the proposed estimator. The bias and variance of both these estimators depend on the autocorrelation function of the input. The expressions for the bias and variance of Denenberg's estimator contain terms similar to those in the expressions for the proposed estimator. In many cases, where (5.37) and (5.39) contain an autocorrelation or cross-correlation function, (5.59) and (5.60) contain the average of that function and its Hilbert transform.

In terms of estimator variance, the performance of Ciciora's device, with a divider appended, depends upon the phase shift of the specialized filter, and is best when the filter has zero phase shift.

The performance of the proposed device is very close to that of Ciciora's, using a divider and a specialized filter of zero phase shift.

The performance of Denenberg's device is better than that of the other two devices. However, for a typical input

signal having a 6 db bandwidth of 60 Hz, and for an averaging time of 1.0 second, the variance of the proposed estimator is 2.8 Hz^2, while that of Denenberg's is 2.66 Hz^2. At $T = 0.1$ second, the proposed estimator has a variance of 32 Hz^2, compared with 26.6 Hz^2 for Denenberg's device.

For very long averaging times, all three estimators are asymptotically perfect. That is, the bias and the variance of each estimate approach zero as T approaches infinity. Furthermore, if the phase shift of Ciciora's specialized filter is zero, then, for <u>any</u> T, all of the estimators are asymptotically perfect as the bandwidth of the input signal approaches zero.

The proposed device should find use in radar meteorology, because it has the advantages of being relatively simple and requiring no difficult-to-synthesize filters.

The following is suggested for future research:

Investigate the possibility of synthesizing, approximately, Ciciora's filter with zero phase shift. Obtain approximate expressions for the bias and the variance of his estimate, in terms of the input autocorrelation function, as was done for the other two devices.

Determine, if possible, the cross-correlation functions at the divider inputs of all three devices, so that the divider analysis of Chapter V can be applied without making use of the power series approximation.

Investigate the possibility of extending the proposed device to estimate the bandwidth, as well as the average frequency, of the input process.

APPENDIX A
THE HILBERT TRANSFORM

Let x(t) be a real function of time. Then the Hilbert transform of x(t), denoted $\check{x}(t)$, is defined by

$$\check{x}(t) = \frac{1}{\pi} \int_{-\infty}^{\infty} \frac{x(\tau)}{t-\tau}\, d\tau \quad . \tag{A-1}$$

Using the convolution notation, this is

$$\check{x}(t) = x(t) * \frac{1}{\pi t} \quad . \tag{A-2}$$

Thus a Hilbert transform has impulse response $h(t) = 1/\pi t$ as shown in Fig. 26.

The transfer function $H(j\omega)$ is found from

$$H(j\omega) = \int_{-\infty}^{\infty} h(t)\, e^{-j\omega t}\, dt$$

$$= \frac{1}{\pi} \int_{-\infty}^{\infty} \frac{e^{-j\omega t}}{t}\, dt \quad . \tag{A-3}$$

Breaking this into two integrals gives

$$H(j\omega) = \frac{1}{\pi} \int_{-\infty}^{0} \frac{e^{-j\omega t}}{t}\, dt + \frac{1}{\pi} \int_{0}^{-\infty} \frac{e^{-j\omega t}}{t}\, dt \quad . \tag{A-4}$$

Substituting $x = -t$ and reversing the limits in the first integral gives

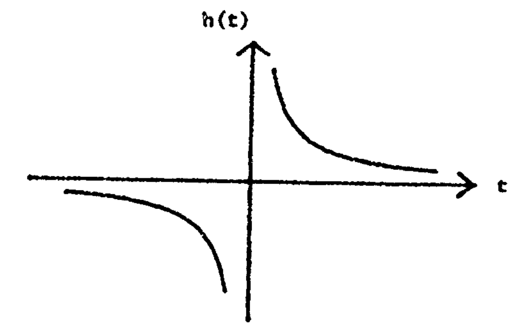

Fig. 26. Impulse Response of a Hilbert Transform Network

$$H(j\omega) = -\frac{1}{\pi} \int_{0}^{\infty} \frac{e^{j\omega x}}{x}\, dx + \frac{1}{\pi} \int_{0}^{\infty} \frac{e^{-j\omega t}}{t}\, dt$$

$$= \frac{1}{\pi} \int_{0}^{\infty} \frac{e^{j\omega t} - e^{-j\omega t}}{t}\, dt \quad . \tag{A-5}$$

Writing this as a sine gives

$$H(j\omega) = \frac{j2}{\pi} \int_{0}^{\infty} \frac{\sin \omega t}{t}\, dt \tag{A-6}$$

For $\omega > 0$,

$$H(j\omega) = \frac{j2}{\pi} \left(\frac{\pi}{2}\right) = j \ , \tag{A-7}$$

while for $\omega < 0$,

$$H(j\omega) = \frac{j2}{\pi} \left(\frac{-\pi}{2}\right) = -j \quad . \tag{A-8}$$

Figure 27 shows the transfer function $H(j\omega)$.

The Hilbert transform of cos ωt is sin ωt for ω 0 and -sin ωt for ω 0.

It can be shown[9] that

$$\check{\check{x}}(t) = -x(t) \ . \qquad \text{(A-9)}$$

The <u>analytic signal</u> associated with $x(t)$ is defined by

$$z(t) = x(t) + j\check{x}(t) \ . \qquad \text{(A-10)}$$

It can be shown[9] that if $S_{xx}(f)$ is the power spectral density of $x(t)$ and $S_{zz}(f)$ is that of $z(t)$, then

$$\begin{aligned} S_{zz}(f) &= 4\,S_{xx}(f) \qquad && f \quad 0 \\ &= 0 && f < 0 \ . \end{aligned} \qquad \text{(A-11)}$$

Thus the analytic signal has a one-sided spectrum.

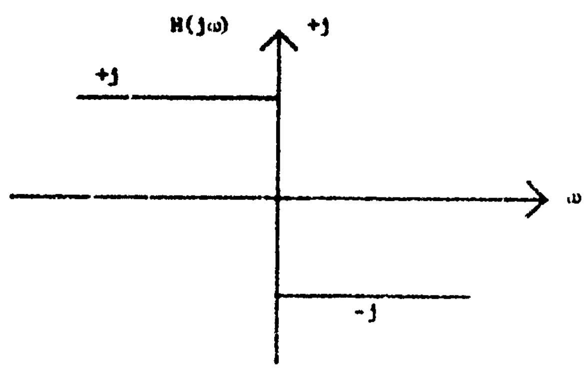

Fig. 27. Transfer Function of a Hilbert Transform Network

APPENDIX B

RAW LAB DATA

In the tables below, N and D represent the numerato. and denominator outputs <u>in millivolts</u>, respectively. In all cases, due to the settings of the potentiometers, D should be multiplied by 0.636. However, if this is not done the results will not change. A new scale will merely be obtained in the calibration curve of Fig. 25.

$T = 1.0$ sec; $\bar{T} = 10{,}000$ Hz; $f_{LO} = 10{,}100$ Hz

Potentiometers set at 299, 134, 132

N	D	N	D	N	D	N	D	N	D
1591	1463	1269	1185	1461	1395	1339	1258	1542	1451
1628	1521	1325	1237	1653	1544	1538	1419	1678	1557
1401	1337	1507	1415	1548	1477	1430	1345	1210	1142
1569	1494	1369	1249	1407	1326	1576	1468	1450	1343
1313	1237	1219	1160	1336	1274	1278	1190	[illegible]	1475
1523	1407	1564	1457	1502	1409	1444	1359	1488	1424
[illegible]	1681	1341	1248	1366	1328	1638	1532	1585	1497
1261	1172	1561	1442	1410	1340	1666	1590	1862	1750
1619	1528	1596	1533	1454	1398	1537	1453	1394	1313
1300	1192	1372	1285	1421	1369	1460	1360	1344	1290
1474	1392	1443	1343	1224	1158	1654	1594	1389	1292
1481	1387	1275	1235	1546	1453	1708	1635	1792	1674
1619	1481	1412	1322	1460	1382	1580	1515	1464	1352
1379	1275	1488	1387	1629	1531	1256	1196	1429	1342
1518	1415	1410	1344	1523	1376	1374	1310	1680	1593
1211	1140	1559	1453	1157	1107	1225	1163	1488	1411
1578	1468	1659	1565	1616	1520	1539	1468	1400	1344
1356	1267	1437	1353	1534	1408	1445	1366	1481	1397
1719	1636	1460	1314	1563	1425	1470	1406	1609	1486
1463	1354	1453	1357	1256	1179	1296	1202	1452	1370

$T = 0.1$ sec; $\bar{f} = 10{,}000$ Hz; $f_{LO} = 10{,}100$ Hz

Potentiometers set at 299, 134, 132

N	D	N	D	N	D	N	D	N	D
2070	1822	1348	1196	2187	1962	1751	1651	1462	1300
1834	1754	1472	1358	1588	1364	2230	1850	2285	2000
1439	1279	881	737	1852	1749	1473	1309	1303	1188
1708	1581	1176	1158	2456	2250	1212	1138	1336	1198
1938	1777	1739	1614	1827	1482	1375	1333	2277	2132
1282	1068	1522	1489	1727	1500	1563	1457	2426	2144
2210	2040	1530	1313	980	870	1646	1464	1536	1315
1423	1332	2188	2036	1495	1355	1245	1076	1715	1638
2200	1953	1356	1184	2362	2414	1156	961	1710	1420
1548	1303	1666	1400	1847	1597	1124	985	1242	1067
2062	1850	1940	1788	2002	1764	1251	1105	1081	942
1665	1600	954	861	871	811	1802	1686	1140	986
1203	1039	2170	1899	1994	1837	1385	1137	1987	1934
1276	1109	1613	1357	927	959	1304	1282	2340	1940
1674	1515	1296	1106	858	332	1979	1776	2547	2290
1318	1248	1438	1288	1633	1436	1975	1678	1275	1118
1917	1775	2016	1925	1273	1225	2284	1935	1742	1570
1915	1734	1327	1184	1484	1383	1345	1253	2048	1637
2679	2199	1454	1353	1213	1062	1902	1770	1004	833
1021	956	1181	1219	2562	2224	1371	1286	1649	1470

$T = 1.0$ sec; $\bar{T} = 10{,}000$ Hz; $f_{LO} = 9{,}900$ Hz

Potentiometers set at 299, 134, 132

-N	D	-N	D	-N	D	-N	D	-N	D
1117	1256	1017	1154	1380	1571	1382	1542	1298	1470
1114	1276	1292	1486	1400	1620	1222	1388	1056	1219
971	1130	1163	1295	1346	1522	1081	1268	1035	1212
968	1088	1037	1231	975	1112	1112	1281	1099	1276
1283	1479	1225	1386	1172	1355	1172	1330	1381	1569
1178	1342	1118	1327	1160	1350	1299	1504	1246	1435
1152	1308	1265	1479	1121	1293	1296	1495	1335	1561
1373	1518	1270	1475	1193	1382	1093	1295	1081	1312
1107	1273	1230	1426	1064	1251	1196	1365	1026	1182
1161	1348	1284	1450	1211	1418	1065	1230	1318	1530

T = 1.0 sec; $\overline{f}$ = 10,000 Hz; f_{LO} = 9,800 Hz

Potentiometers set at 299, 134, 069

-N	D	-N	D	-N	D	-N	D	-N	D
1323	1409	1241	1321	1466	1570	1262	1357	1282	1362
1474	1568	1364	1454	1438	1536	1306	1380	1526	1611
1475	1567	1445	1536	1479	1572	1298	1373	1311	1389
1369	1461	1419	1529	1265	1322	1289	1364	1304	1403
1306	1382	1492	1565	1120	1235	1576	1463	1264	1323
1171	1243	1433	1533	1581	1675	1346	1433	1397	1465
1225	1304	1319	1395	1414	1484	1346	1438	1473	1564
1131	1202	1450	1545	1249	1332	1389	1457	1367	1458
1475	1592	1302	1393	1680	1788	1488	1554	1396	1479
1493	1594	1219	1296	1267	1331	1591	1693	1405	1506

T = 1.0 sec; $\overline{f}$ = 10,000 Hz; f_{LO} = 10,200 Hz

Potentiometers set at 299, 134, 069

N	D	N	D	N	D	N	D	N	D
1358	1228	1534	1395	1477	1339	1769	1604	1861	1664
1816	1627	1729	1542	1630	1466	1688	1534	1704	1528
1371	1236	1619	1403	1504	1383	1692	1505	1803	1645
1733	1546	1598	1438	1796	1605	1889	1723	1451	1311
1897	1692	1997	1791	1672	1502	1387	1692	1950	1415
1875	1679	1582	1415	1639	1476	1999	1789	1555	1397
2061	1865	1796	1619	1632	1470	1770	1536	1561	1383
1795	1607	1706	1507	1651	1493	1907	1716	1767	1615
1442	1295	1481	1322	2021	1812	1685	1529	1739	1562
1748	1552	1790	1622	1712	1539	1735	1560	1724	1564

T = 1.0 sec; $\overline{f}$ = 10,000 Hz; f_{LO} = 9,950 Hz

Potentiometers set at 299, 134, 132

-N	D	-N	D	-N	D	-N	D	-N	D
484	1338	483	1288	487	1258	666	1806	593	1491
537	1504	548	1476	464	1341	523	1344	635	1624
440	1204	612	1553	495	1304	606	1645	555	1364
524	1377	490	1253	587	1575	517	1335	590	1581
570	1561	624	1679	523	1386	518	1374	671	1703
530	1352	466	1259	608	1565	679	1670	559	1446
522	1478	456	1159	566	1557	539	1391	658	1655
537	1450	585	1580	587	1515	551	1499	612	1533
522	1317	458	1267	594	1514	565	1435	560	1457
639	1204	541	1165	585	1638	585	1540	584	1529

T = 1.0 sec; $\overline{f}$ = 10,000 Hz; f_{LO} = 10,050 Hz

Potentiometers set at 299, 134, 132

N	D	N	D	N	D	N	D	N	D
887	1484	976	1671	950	1661	962	1731	730	1343
888	1520	804	1465	796	1465	853	1492	669	1202
1029	1833	956	1635	889	1550	874	1486	912	1533
822	1429	846	1484	791	1395	880	1558	836	1530
772	1343	311	1443	841	1489	858	1464	957	1639
866	1478	944	1624	726	1284	991	1793	[illegible]	1554
898	1601	844	1416	810	1404	834	1542	[illegible]	1547
843	1441	797	1410	773	1348	920	1501	359	1459
877	1541	839	1385	802	1423	928	1497	935	1642
843	1432	1048	1737	1036	1744	757	1306	[illegible]	1360

T = 1.0 sec; $\overline{f}$ = 10,000 Hz; f_{LO} = 9,975 Hz

Potentiometers set at 299, 134, 378

-N	D	-N	D	-N	D	-N	D	-N	D
874	1590	843	1605	1069	1695	892	1450	746	1549
1032	1667	861	1542	1041	1719	908	1612	912	1404
791	1313	810	1328	970	1521	925	1551	709	[illegible]
967	1524	922	1611	804	1606	747	1413	950	[illegible]
876	1600	832	1485	899	1687	1009	1634	886	[illegible]
894	1412	843	1499	783	1437	823	1551	752	1659
709	1296	1047	1944	971	1612	949	1639	874	1711
817	1567	750	1202	839	1644	875	1473	973	1579
954	1805	838	1353	792	1337	975	1592	860	1516
811	1693	891	1722	768	1425	861	1483	1002	1652

T = 1.0 sec; $\overline{f}$ = 10,000 Hz; f_{LO} = 10,025 Hz

Potentiometers set at 299, 134, 378

N	D	N	D	N	D	N	D	N	D
1124	1397	1367	1652	1133	1278	1369	1671	[illegible]	[illegible]
1425	1632	1477	1601	1109	1365	1463	1624	1283	1530
1336	1624	1244	1399	1171	1334	1234	1521	1373	1548
1524	1647	1525	1750	1206	1469	1228	1570	1139	1312
1158	1542	1175	1264	1166	1483	1092	1465	1226	1506
1437	1650	1206	1517	1437	1637	1004	1394	1113	1412
1337	1377	1070	1335	1184	1493	1237	1512	1076	1363
1356	1677	1253	1581	1415	1469	1282	1478	1365	1652
1072	1305	1372	1567	1224	1451	1086	1343	1221	1436
1407	1778	1179	1436	1349	1566	1276	1568	1507	1745

BIBLIOGRAPHY

1. Bello, P. A. "Some Techniques for the Instantaneous Real-Time Measurement of Multipath and Doppler Spread," IEEE Transactions on Communication Technology, Vol. 13, No. 3, September 1965, pp. 185-192.

2. Ciciora, W. S. A Method of Average Frequency Measurement, Ph.D. Thesis, Illinois Institute of Technology, June 1969.

3. Davenport, W. B. and W. L. Root, An Introduction to the Theory of Random Signals and Noise, McGraw-Hill Book Company, Inc., New York, 1958, p. 168.

4. Ibid., p. 69.

5. Denenberg, J. N. The Estimation of Spectral Moments, Ph.D. Thesis, Illinois Institute of Technology, May 1971.

6. Ibid., p. 27.

7. Ibid., p. 50.

8. Miller, M. S. and M. M. Rochwarger, "On Estimating Spectral Moments in the Presence of Colored Noise," IEEE Transactions on Information Theory, Vol. IT-16, No. 3, May 1970, pp. 303-309.

9. Papoulis, A. Probability, Random Variables, and Stochastic Processes, McGraw-Hill Book Company, Inc., New York, 1965, p. 357.

10. Ibid., p. 317.

11. Ibid., p. 352.

12. Systems Analysis and Additional Instrumentation for Modified "Porcupine" C-Band Pulse Doppler Radar, Raytheon Company, Equipment Division, Wayland Laboratories, Wayland, Massachusetts, December 30, 1966.

LAP PUBLICATIONS LIST

Prior to July 1968, LAP reports were listed under the "Remote Atmospheric Probing Project" or RAPP. Whenever a report has been published in a scientific journal, the journal reference is given in parenthesis.

Technical Reports

No. 1. Atlas, D., K. Naito and R. E. Carbone, 1967: Bistatic microwave probing of a refractively perturbed clear atmosphere. RAPP. (J. Atmos. Sci., 25, 257-268 (1968)).

No. 2. Srivastava, R. C. and D. Atlas, 1967: Growth, motion and concentration of precipitation particles in convective storms. RAPP. (J. Atmos. Sci., 26:535-544 (1969)).

No. 3. Sloss, P. W. and D. Atlas, 1968: Wind shear and reflectivity gradient effects on Doppler radar spectra. RAPP. (J. Atmos. Sci., 25:1080-1089 (1968)).

No. 4. Atlas, D. and R. Tatehira, 1968: Precipitation-induced mesoscale wind perturbations in the melting layer. RAPP. (Quart. J. Roy. Met. Soc., 95:544-560 (1969)).

No. 5. Srivastava, R. C., D. Atlas, R. Tatehira, W. Marker, Jr. and R. E. Carbone, 1968: Temperature, pressure, and wind perturbations produced by melting snow. RAPP. (Quart. J. Roy Met. Soc., 95:544-560 (1969)).

No. 6. Srivastava, R. C. and R. E. Carbone, 1968: Statistics of instantaneous frequency and amplitude as related to the Doppler spectrum. RAPP. (Radio Science, 4:381-393 (1969)).

No. 7. Tatehira, R. and R. C. Srivastava, 1968: Methods of updraft estimation with Doppler radar. RAPP. (Proceedings Thirteenth Radar Meteorology Conference, McGill University, Montreal, Canada 20-23 August 1968, pp. 36-43).

No. 8. Atlas, D., R. C. Srivastava, R. E. Carbone and D. H. Sargeant, 1969: Doppler crosswind relations in radio tropo-scatter beam swinging for a thin scatter layer. LAP. (J. Atmos. Sci., 26:1104-1117 (1969)).

No. 9. Atlas, D., R. C. Srivastava and W. S. Marker, Jr., 1969: The influence of specular reflections on bistatic tropospheric radio scatter from turbulent strata. LAP. (J. Atmos. Sci., 26: 1118-1121 (1969)).

No. 10. Atlas, D., 1969: The measurement of crosswind by non-coherent dual arm bistatic radio tropo-scatter techniques. LAP. (J. Atmos. Sci., 26:1122-1127 (1969)).

Technical Reports (cont.)

No. 11. Srivastava, R. C., 1969: Note on the theory of growth of cloud drops by condensation. LAP. (J. Atmos. Sci., 26:776-780 (1969)).

No. 12. Sekhon, R.S. and R.C. Srivastava, 1969: Snow size spectra and radar reflectivity. LAP. (J. Atmos. Sci., 27:299-307 (1970)).

No. 13. Atlas, D., J.H. Richter and E.E. Gossard, 1969: Waves, turbulence, and insects as seen by ultra high resolution radar. LAP.

No. 14. Eccles, P.J. and D. Atlas, 1969: A dual wavelength radar hail detector. LAP.

No. 15. Atlas, D. and R. C. Srivastava, 1969: A method for radar turbulence detection. LAP. (IEEE Trans. AES-7:179-187(1971)).

No. 16. Ekpenyong, B.E. and R.C. Srivastava, 1970: Radar characteristics of the melting layer -- A theoretical study. LAP.

No. 17. Atlas, D., F.I. Harris and J. H. Richter, 1970: The measurement of point target speeds with incoherent non-tracking radar: Insect speeds in atmospheric waves. LAP. (J. Geophys. Res., 75:7588-7595 (1970)).

No. 18. Sekhon, R.S. and R.C. Srivastava, 1970: Doppler radar observation of drop-size distribution in a thunderstorm. LAP. (J. Atmos. Sci., 28, 983-994 (1971))

No. 19. Atlas, D. and J. I. Metcalf, 1970: The amplitude and energy of breaking Kelvin-Helmholtz waves and turbulence. LAP

No. 20. Srivastava, R.C. and R. E. Carbone, 1971: The effect of signal fluctuations on the performance of dual wavelength radar hail detector. LAP.

No. 21. Stratmann, E., D. Atlas, J.H. Richter and D.R. Jensen, 1971: Sensitivity calibration of a dual beam vertically pointing FM-CW radar. LAP.(J. Applied Meteor., 10, 1260-1265 (1971))

No. 22. Atlas, D., R.C. Srivastava, and R.S. Sekhon, 1971: Doppler radar characteristics of precipitation at vertical incidence. LAP. (Submitted to Reviews in Geophysics).

No. 23. Dennenberg, J. N., 1971: The estimation of spectral moments. LAP.

No. 24. Carbone, R.E., 1971: One-dimensional numerical simulation of a dual wavelength radar hail detector. LAP.

Technical Reports (cont.)

No. 25. Carbone, R. E., 1972: A two-dimensional evaluation of a dual wavelength radar hail detector. LAP.

No. 26. Serafin, R. J., 1972: Radar measurement of the atmospheric turbulence structure function. LAP.

No. 27. Srivastava, R. C. and D. Atlas, 1972: Effect of finite radar pulse volume on turbulence measurements. LAP.

No. 28. Metcalf, J. I. and D. Atlas, 1972: Microscale ordered motions and atmospheric structure associated with thin echo layers in stable stratified zones. LAP.

No. 29. Sychra, J., 1972: On the theory of pulse volume filtering of turbulent reflectivity and velocity fields. LAP.

No. 30. Atlas, D., R. S. Sekhon and R. J. Serafin, 1972: Doppler turbulence measurements in an evaporating 'stalactite' cloud base zone. LAP.

No. 31. Nerro, J. J., 1973: Estimation of the average frequency of a random process. LAP.

Technical Notes

No. 1. Atlas, D., 1968: Clear air turbulence detection methods: A review. RAPP. (Proc. Conf. on Clear Air Turbulence and Its Detection. Boeing Scientific Res. Lab., Aug. 14-16, 1968, Plenum Press, Eds., Y-H. Pao and A. Goldburg, 1969, pp. 381-401).

No. 2. Atlas, D., 1968: Radar probing of atmospheric turbulence: A prospectus. LAP.

No. 3. Atlas, D., 1968: Weather radar for the supersonic transport. LAP.

No. 4. Atlas, D., 1969: Progress in radar and bistatic radio tropo-scatter from the atmosphere - 1969. LAP.

No. 5. Laboratory for Atmospheric Probing, 1970: Papers presented at the Fourteenth Radar Meteorology Conference, Tucson, Arizona, 17-20 November 1970.

No. 6. Stratmann, E. and J. I. Metcalf, 1971: Digital processing of FM-CW radar data. LAP. J. Applied Met., 10:1260-1265.

No. 7. Laboratory for Atmospheric Probing, 1972: Papers presented at the Fifteenth Radar Meteorology Conference, Champaign-Urbana, Illinois, 10-12 October 1972.

Other Journal Articles

Atlas, D., 1969: Further remarks on atmospheric probing by ultra-sensitive radar. Atmospheric Exploration by Remote Probes. Report of the Panel on Remote Atmospheric Probing, Vol. 2., U. S. National Academy of Science, Comm. on Atmos. Sci., pp. 243-252.

Atlas, D., 1969: Radar and bistatic radio techniques. Atmospheric Exploration by Remote Probes. Report of the Panel on Remote Atmospheric Probing, Vol. 1. U. S. National Academy of Sciences, Comm. on Atmos. Sci., pp. 15-26.

Srivastava, R. C., 1969: Note on the theory of growth of cloud drops by condensation. J. Atmospheric Sci., 26, 776-780.

Harris, F. K., B. Ekpunyong, D. Atlas and R. Serafin, 1970: Doppler winds, stalactites, and secondary generators at the evaporation base of an ice crystal overcast. Preprints of Papers presented at the 14th Radar Meteorology Conference, Nov. 17-20, 1970, Tucson, Arizona, pp. 181-186.

Srivastava, R. C., 1971: Size distribution of raindrops generated by their breakup and coalescence. J. Atmospheric Sci., 28, 410-415.

Yang, C. Y. and L. C. Peach, 1972: Incoherent radar measurement of atmospheric turbulence. Preprints of Papers presented at the 15th Radar Meteorology Conference, October 10-12, 1972, Champaign-Urbana, Illinois, pp.

Serafin, R. J., L. C. Peach and D. Atlas, 1972: Radar measurement of the atmospheric turbulence structure function. Preprints of Papers presented at the 15th Radar Meteorology Conference, October 10-12, 1972, Champaign-Urbana, Illinois, pp.

Denenberg, J. N., R. J. Serafin and L. C. Peach, 1972: Uncertainties in coherent measurement of the mean frequency and variance of the Doppler spectrum from meteorological echoes. Preprints of Papers presented at the 15th Radar Meteorology Conference, October 10-12, 1972, Champaign-Urbana, Illinois, pp.

Miscellaneous Unpublished Papers

Atlas, D., 1968: Radar measurement of precipitation: A review and critique. Paper presented at the 13th Radar Meteorology Conf., McGill Univ., Montreal, Canada, Aug. 20-23, 1968.

Atlas, D., 1969: An overview of remote atmospheric probing techniques. Paper presented at the 49th Annual Meeting of the American Meteorology Society, Jan. 20-23, 1969, New York, N.Y.